A numerical investigation for a source inverse problem in linear acoustics

Marc Bonnet

A numerical investigation for a source inverse problem in linear acoustics

Marc Bonnet

Laboratoire de Mécanique des Solides (centre commun CNRS - X - Mines - Ponts), Ecole Polytechnique, 91128 Palaiseau Cedex, France

Résumé. — On considère le problème de l'identification de la vitesse normale d'une structure vibrante à partir de mesures du champ de pression rayonné. Dans un premier temps, des indications qualitatives sur ce problème inverse sont obtenues sur le cas particulier de la sphère vibrante, pour laquelle la pression rayonnée est connue analytiquement. Ensuite, dans le but de traiter une surface quelconque, on développe certains aspects algébriques de la méthode d'inversion gaussienne, dans le but d'étudier la stabilisation de l'inversion et certains indicateurs de confiance; le problème direct discrétisé est alors construit par la méthode des éléments finis de frontière. On présente enfin des résultats numériques, afin de mettre en évidence l'influence sur l'inversion de certains facteurs: informations *a priori*, mesures perturbées, élimination algorithmique des mesures aberrantes.

Abstract. — We are interested in reconstructing the normal velocity of a vibrating body using measured values of the radiated pressure field. Firstly, some qualitative informations about the behaviour of this inverse problem are obtained through the examination of the particular case of the vibrating sphere, using its well-known analytical solution. Then, as we wish to deal with a vibrating body of arbitrary shape, we develop some algebraic features of the so-called Gaussian inversion method in order to stabilize the inversion and obtain confidence indicators on the result; in this case the direct problem is discretized using the boundary element method. Finally some numerical results are presented in order to highlight the influence of several factors on the result: *a priori* informations, noisy experimental data, detection and elimination of erroneous data, if any.

Inroduction.

This paper deals with the problem of evaluating the normal velocity field U on a vibrating structure (which is represented from the standpoint of acoustical radiation by a closed vibrating surface S) through the knowledge of measured values of the radiated pressure field p; the vibration of S

is assumed to radiate in an infinite space filled with an acoustical fluid (air) of specific mass ρ and sound wave velocity c. Several recent papers have been devoted to this inverse problem sometimes called "acoustic holography". The first studies consider coordinate systems for which the Helmholtz equation is separable (cartesian, cylindrical, spherical, ...), and geometrical configurations such that both the vibrating surface and the measurement points are located on coordinate surfaces. In this case, the wave field is analytically expanded in terms of functions of two coordinates associated to a family of separable surfaces and propagated along the third coordinate in order to relate the measured pressures and the normal velocities [1]. More recently, other studies (see e.g. [2, 3] for arbitrary 3D and axisymmetric vibrating surfaces respectively) deal with arbitrary non-separable geometries, the relation between the exterior pressure field and the normal velocity on S being derived, in a discrete form, from the well-known boundary integral equations and boundary integral representation formulae of linear acoustics (for further reference about boundary integral equations in acoustics and engineering science see for example [4-7] and the references herein). These two approaches are considered in [8, 9] for plane holography problems.

The present work pursues the latter line. Its initial motivation is the integration of the inversion algorithm into a treatment process which would allow one to estimate the mechanical loadings acting on vibrating structures, given measured values of the radiated pressure field. We consider here the above-stated inverse problem from the point of view of the inversion methodology. Accordingly we study some algorithmic details and propose several improvements for a certain approach devoted to the numerical solution of linear ill-posed problems, namely the "Gaussian inversion", which we apply here in the framework of acoustical radiation in an infinite space.

The Gaussian inversion is initially derived by Tarantola as a particular case of his concept of "stochastic inversion" in his textbook devoted to inverse problems [10]. We view this approach as an alternative to the singular value decomposition method which has been used in the works [2] [3] mentioned above to solve numerically the inversion problem. The Gaussian inversion method, which incorporates *a priori* information, is stable with respect to data noise. Furthermore the Gaussian framework involves covariance operators, thus allowing the derivation of easily interpretable confidence or dispersion indicators associated to the numerical solution. Accordingly we investigate here some algorithmic features and improvements for this method. First, as we are interested here in solving inverse problems involving complex-valued data, unkowns and operators, we work out the proper meaning of some quantities involved in the Gaussian inversion process, especially the covariance matrices associated to complex random variables. Then we give some algebraic developments leading to the following improvements of the Gaussian inversion strategy: evaluation of the influence of a single datum on the inversion result, numerical computation of confidence indicators and *a posteriori* detection of outliers in the data set, all of them requiring only a moderate additional computer time cost.

An inversion software, which incorporates the above-mentioned algebraic developments, has been written as a part of the present work.

In the first part of this paper, we state the inverse problem and highlight its ill-posedness using the analytical solution available for the particular case of the vibrating sphere. The improvements of the Gaussian inversion method are the subject of part two, part three being devoted to the results of numerical tests.

1. Inversion of pressure field measurements: statement of the problem.

1.1 Analysis of the particular case of the exterior radiation from a vibrating sphere.

— We consider the particular case of a vibrating sphere S of radius a, centered at the origin O of a spherical coordinates system (O, $\mathbf{r}$, θ, ϕ) (see Fig. 1), for which the radiated pres-

sure field p in the exterior free-space can be analytically expressed in terms of the normal velocity U on S. Accordingly let the surface S vibrate with a given normal velocity $U(\theta, \phi, t)$. We restrict the vibratory motion of S to be axisymmetrical with respect to the polar axis **Oz** (see Fig. 1) and time-harmonic, that is:

$$U(\theta, \phi, t) = U(\phi)e^{-i\omega t}; \qquad p(r, \theta, \phi, t) = p(r, \phi)e^{-i\omega t} \tag{1.1}$$

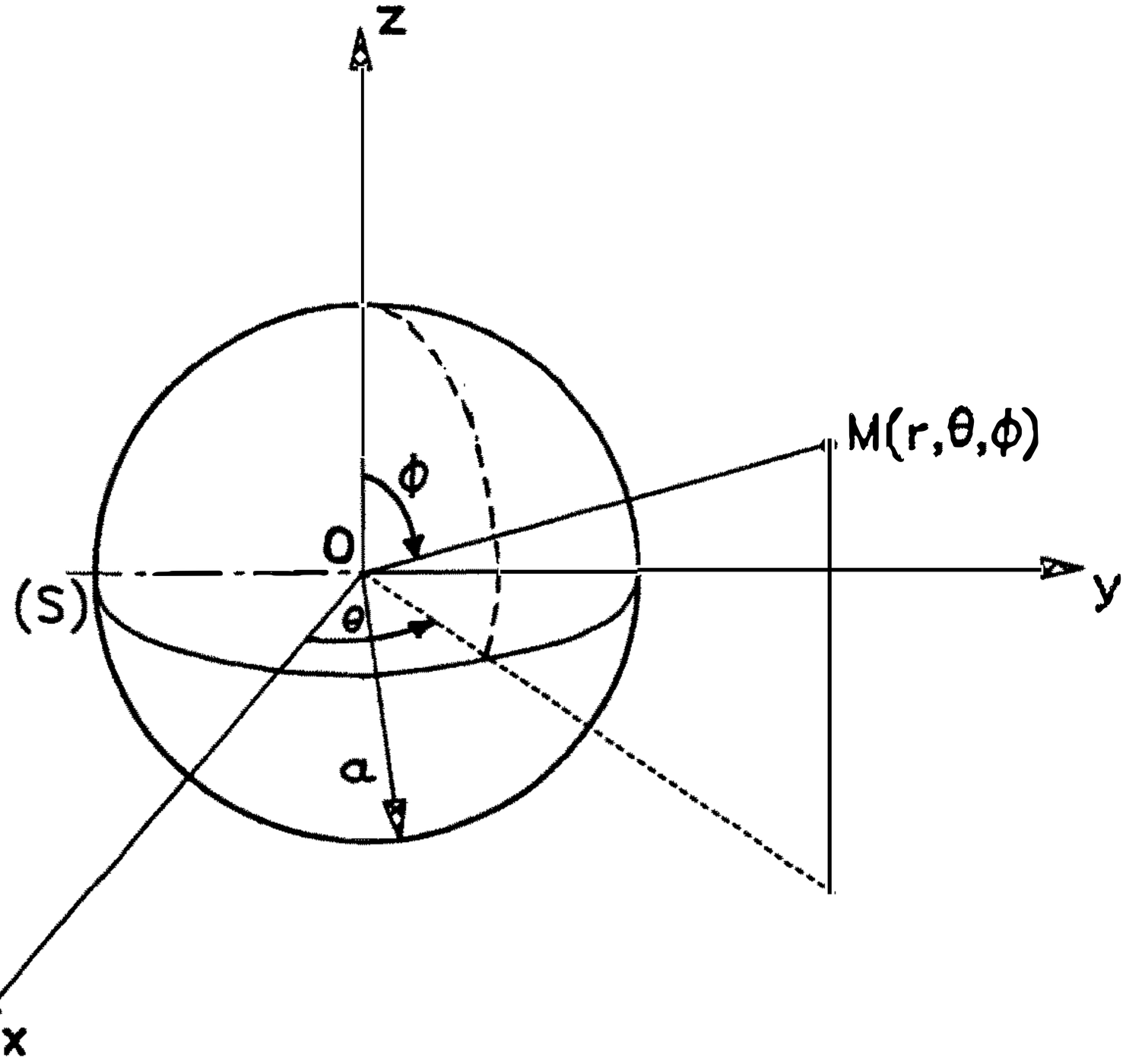

Fig. 1. — The vibrating sphere problem: geometrical configuration.

1.1.1 *General solution for the axisymmetrical vibration of a sphere* [13]. — Under these requirements, $U(\phi)$ can be expanded on the Hilbert orthogonal family of Legendre polynomials $\{(P_\ell)\ , \ell \in \ell\}$:

$$U(\phi) = \sum_{\ell \geq 0} U_\ell P_\ell(\cos\phi); \qquad U_\ell = \frac{2\ell+1}{2}\int_0^\pi U(\phi)P_\ell(\cos\phi)\mathrm{d}\phi \tag{1.2}$$

Accordingly the pressure field $p(r,\ \phi)$ associated to U, which satisfies the Helmholtz equation, is given by:

$$p(r,\ \phi) = \sum_{\ell \geq 0} A_\ell P_\ell(\cos\phi)h_\ell(kr) \qquad (r \leq a) \tag{1.3}$$

in which $h_\ell(kr)$ is the *spherical Hankel function*, of first kind and order ℓ. The coefficients A_ℓ in the expansion (1.3) are related to the U_ℓ through:

$$a_\ell = \frac{\rho c U_\ell}{B_\ell e^{-i\delta_\ell}} \quad \text{with} \quad B_\ell = \left|\frac{\mathrm{d}}{\mathrm{d}z}h_\ell(z)\right|$$

$$\frac{\mathrm{d}}{\mathrm{d}z}h_\ell(z) = B_\ell \mathrm{e}^{\mathrm{i}(\delta_\ell - \pi/2)}\,; \qquad z = ka = 2\pi\frac{a}{\lambda} \tag{1.4}$$

which define B_ℓ and δ_ℓ. Thus the ratio of the moduli of A_ℓ and U_ℓ is equal to an "amplification factor" $\rho c/B_\ell$.

1.1.2 *Amplification factors relating U and p.* — Equation (1.4) allows us to obtain some qualitative information about the infinite-dimensional inverse problem by examinating the amplification factor $\rho c/B_\ell$ relating A_ℓ to U_ℓ, which is plotted against ℓ and for several fixed values of ka in figure 2. One can see that this factor decreases to zero as ℓ increases, this decrease being sharper for smaller values of ka. This means that, for equal amplitudes, the higher-order spherical modes of the normal velocity U produce radiated pressures of lower absolute values, and therefore are more difficult to "see", from measured values of p, than the lower-order ones.

Besides it is possible to show, using the first term of the asymptotic expansion of $h_\ell(ka)$ for ℓ large compared to ka (see [14], among others), that the coefficient $\rho c/B_\ell$ decreases exponentially with ℓ for large values of ℓ.

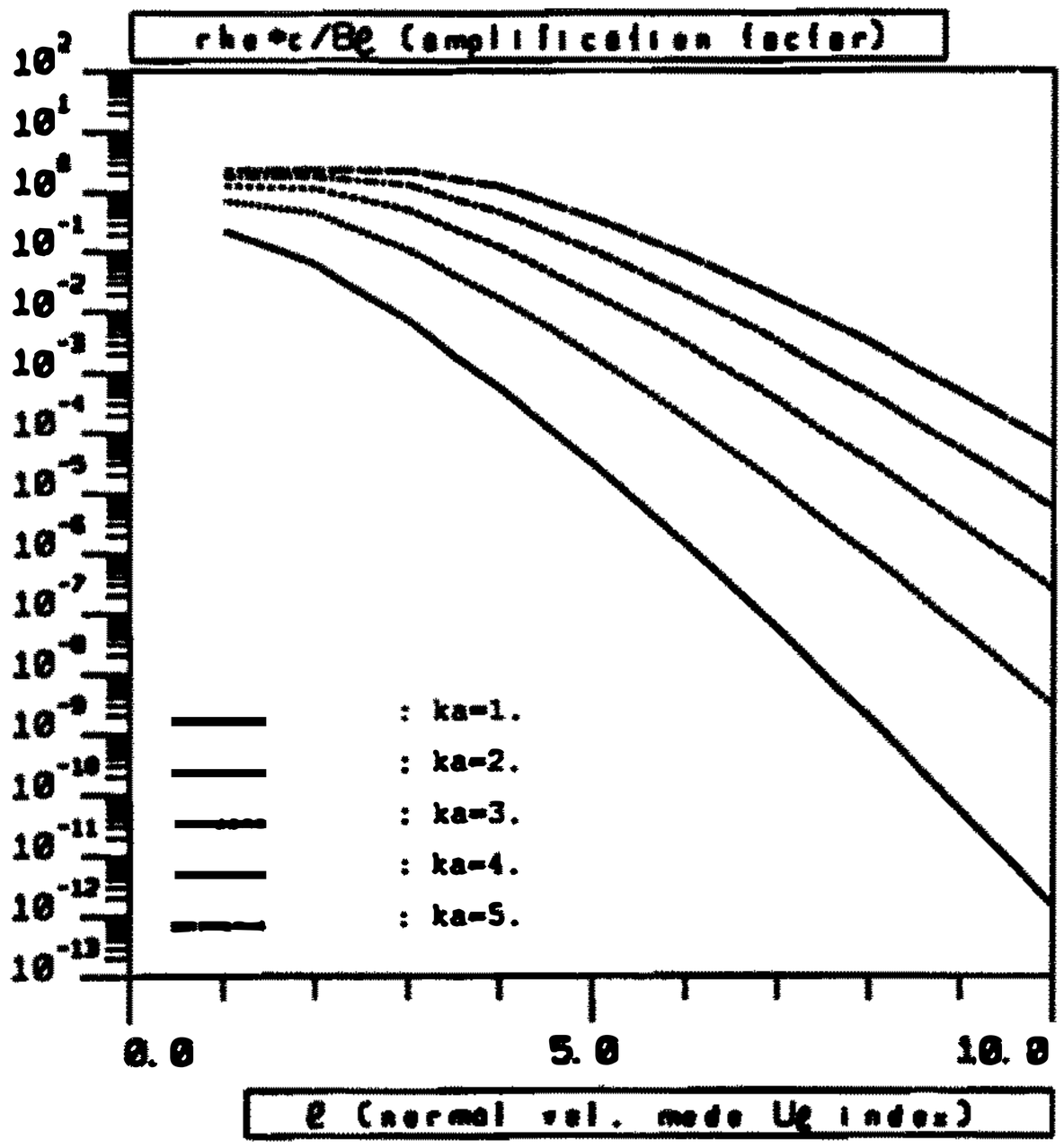

Fig. 2. — Modulus of amplification coefficients $\rho c/B_\ell$ plotted against ℓ, for several values of ka.

1.1.3 *Study of the matrix relation between* $[U_j]_{j=1,\ \ldots,\ n}$ and $[p_i]_{i=1,\ \ldots,\ m}$. — Assume that measured values p_i of p are given at m points $\mathrm{M}_i(r_i, \theta_i, \phi_i)$. These values p_i are linearly related to the coefficients U_j which define the normal velocity on S, using equation (1.3):

$$p_i = \sum_{j \geq 0} G_{ij} U_j \qquad \text{with} \qquad G_{ij} = \frac{\rho c}{B_j} P_j(\cos\phi_i)\, h_j(kr_i) \tag{1.5}$$

Let the convergent infinite summation in (1.5) be truncated at $j = n$, n being an arbitrary truncation level. The truncated summation (1.3) can then be written in a matricial form $\mathbf{p} = \mathbf{GU}$, $\mathbf{G}$

being a complex $m \times n$ matrix, and we investigate now the behaviour of this matrix **G**. Accordingly we apply to **G** the singular value decomposition (see [11] and the references mentioned herein) and examine the singular values $\lambda_1, \ldots, \lambda_n$ of **G**, ordered in decreasing moduli, using subroutine CSVDC of the LINPACK software library [15].

An extensive parameteric study of the numerical behaviour of **G** is difficult to achieve due to the large number of relevant factors: for example one should examine the influence of the spatial location of the measurement points M_i, which demands a great deal of compositions. So we limited ourselves to examine the influence of the frequency, the distance of the measurement points M_i to the center of the sphere and the number of unknowns and of measurement points, judging that such partial results would be representative of the behaviour of the inverse problem under more general conditions. We proceed in presenting some numerical results related to the study of **G**.

• Singular values of G. — In figure 3 the moduli $|\lambda_\ell|$ of the singular values are plotted against their index ℓ; one can see their very fast decay. The singular values were computed for six different sets of $m = 10$ measurement points, the points of a set being all located at the same distance r to the center of the vibrating sphere, with $n = 10$ and $ka = 1.$; r varying from one curve to another.

In figure 4 the moduli of the singular values are again plotted against their index but this time for sets of measurement points being located at the same distance r to the center of the vibrating sphere but of different sizes ($m = 20,\ 30,\ 40,\ 50$ points), with $n = 10$, $ka = 1$ and $kr = 2$; m varying from one curve to another. We see that the modulus of the singular value increases with m for a fixed number n of unknowns.

Examination of figures 3 and 4 shows that the modulus of λ_ℓ behaves roughly like $\exp(-\ell)$.

• Condition number of G. — It is defined as the ratio: $\mathrm{Cond}(\mathbf{G}) = |\lambda_1| / |\lambda_n|$. We numerically evaluated Cond (**G**) against ka (r being fixed) (Fig. 5) and against kr (ka being fixed) (Fig. 6). In these figures one sees that Cond (**G**) is a decreasing function of the nondimensional frequency ka and an increasing fonction of the distance r of the measurement points to the center of S. For the results of figures 5 and 6 we set $m = n = 10$, which is a rather small value, but one can see that Cond(**G**) takes quite high values compared to the size of **G**, especially for ka small or r/a large. Furthermore, our numerical experiments showed that the value of Cond(**G**) is hardly affected by increasing the number m of measurement points as was done for figures 3 and 4.

These preliminary results show the ill-conditioned character of the inverse problem for a general vibrating surface. This point motivates the use of an inverse problem numerical approach and will be confirmed by the numerical results presented in section 3.

1.2 FORMULATION OF THE INVERSE PROBLEM FOR AN ARBITRARY VIBRATING SURFACE. — Now we consider an arbitrary closed surfaces subjected to a vibratory motion, U being the normal velocity field on S. The pressure field $p|\mathbf{x}|$ satisfies, for every fixed point $\mathbf{x} = (x_1,\ x_2,\ x_3)$ of S, the following integral equation:

$$p(\mathbf{x}) + \int_S [p(\mathbf{y}) - p(\mathbf{x})] n_s(\mathbf{y}) \frac{\partial}{\partial y_s} G(\mathbf{x}, \mathbf{y}) \mathrm{d}S_\mathbf{y} + \frac{i}{\omega\rho} \int_S U(\mathbf{y}) G(\mathbf{x}, \mathbf{y}) \mathrm{d}S_\mathbf{y} = 0 \qquad (1.6)$$

with $\qquad G(\mathbf{x}, \mathbf{y}) = (e^{ikr}) / 4\pi r \ ; \ r = \|\mathbf{y} - \mathbf{x}\| \qquad \forall x \in \mathbb{R}^3$

which is a regularized version [17] of the classical integral equation obtained using Green's third identity; the function $G(\mathbf{x}, \mathbf{y})$ in equation (1.6) above is the Green function associated to the Helmholtz equation. When one considers, as in the present work, the acoustic radiation in the free space outside a vibrating closed surface S, the unit normal $\mathbf{n}(\mathbf{y}) = (n_1,\ n_2,\ n_3)$ at the current

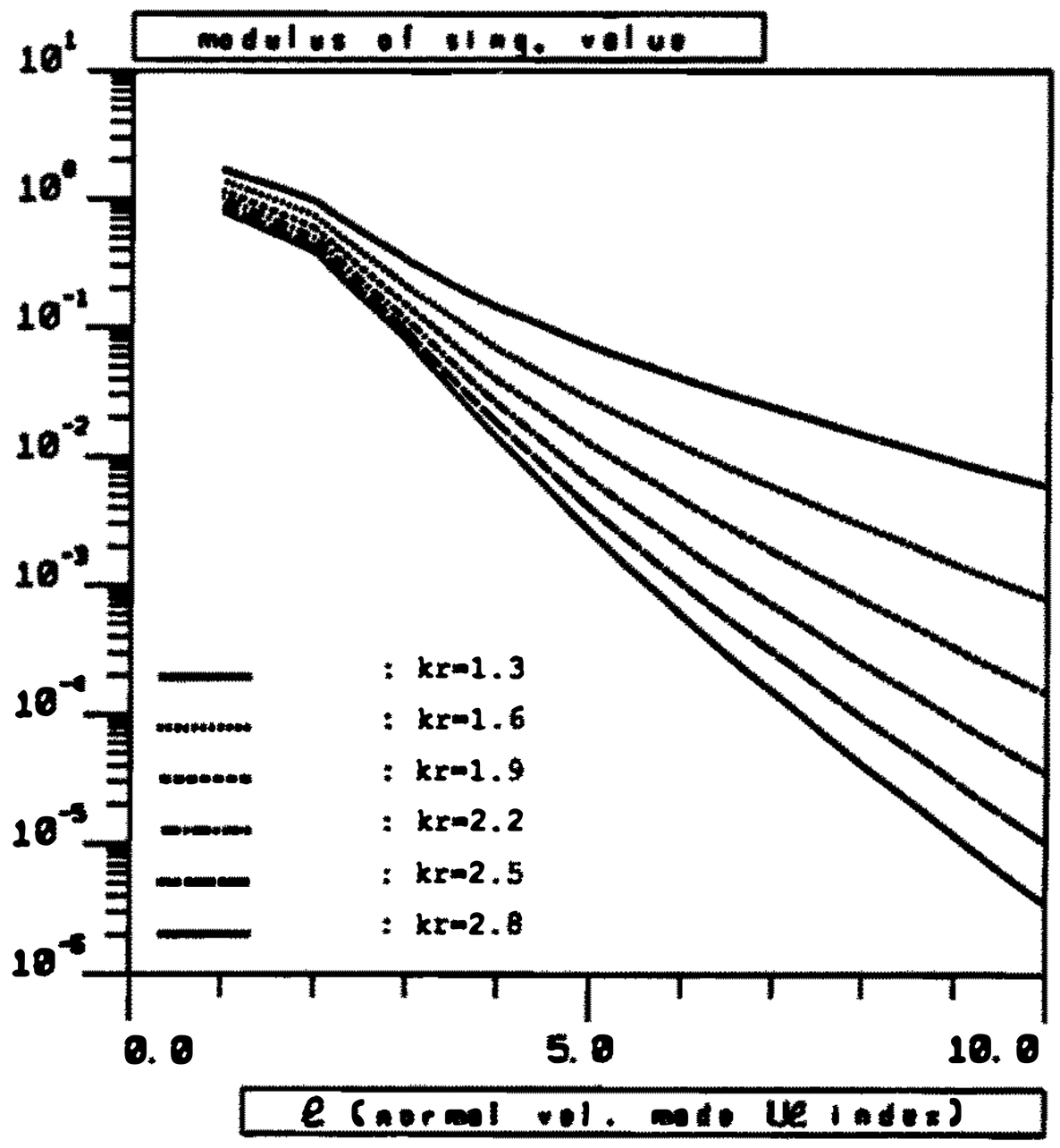

Fig. 3. — $|\lambda_\ell|$ plotted against ℓ for several values of r (r being the distance of the measurement points to the origin O).

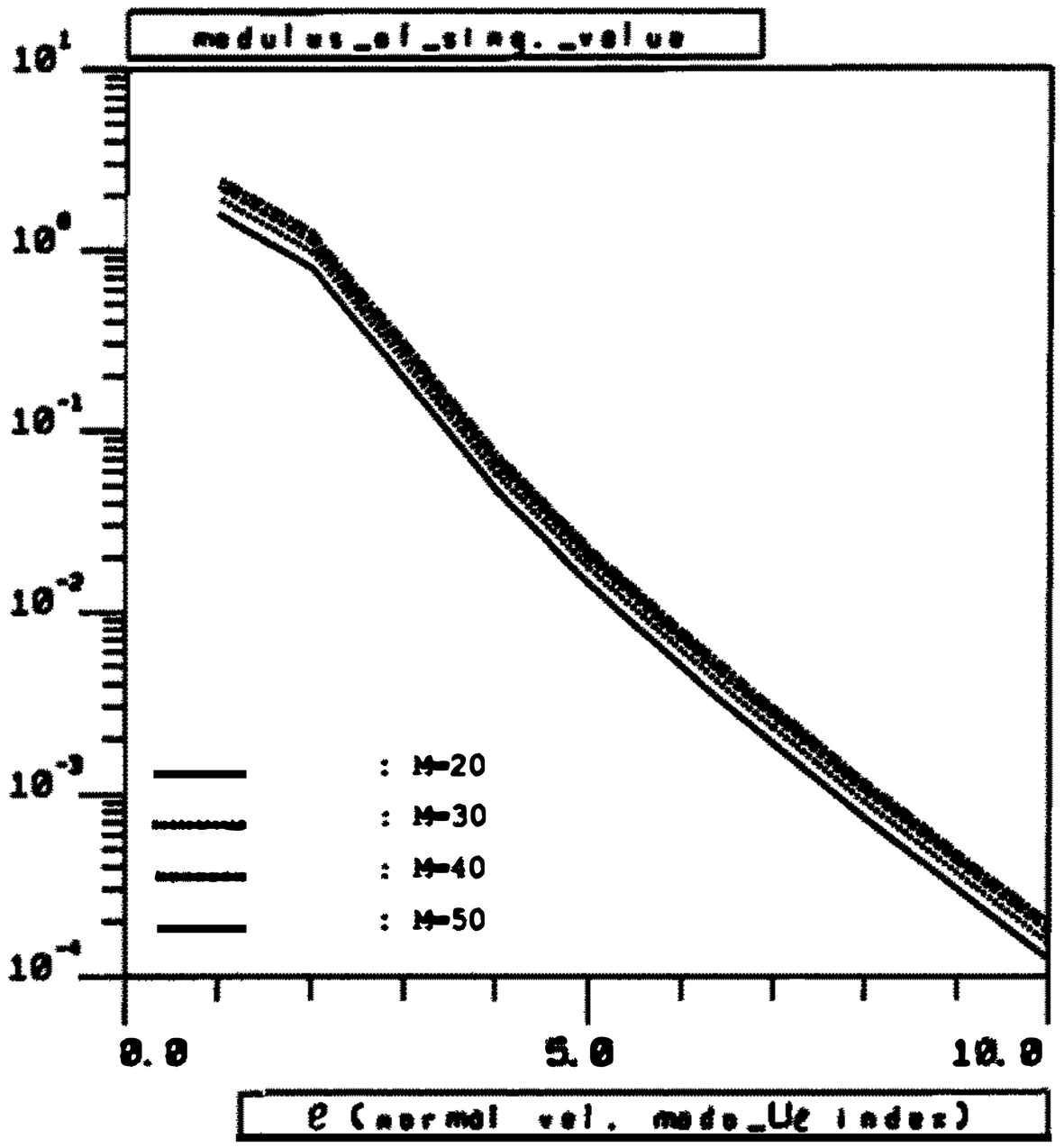

Fig. 4. — $|\lambda_\ell|$ plotted against ℓ for several values of the number M of measurements points.

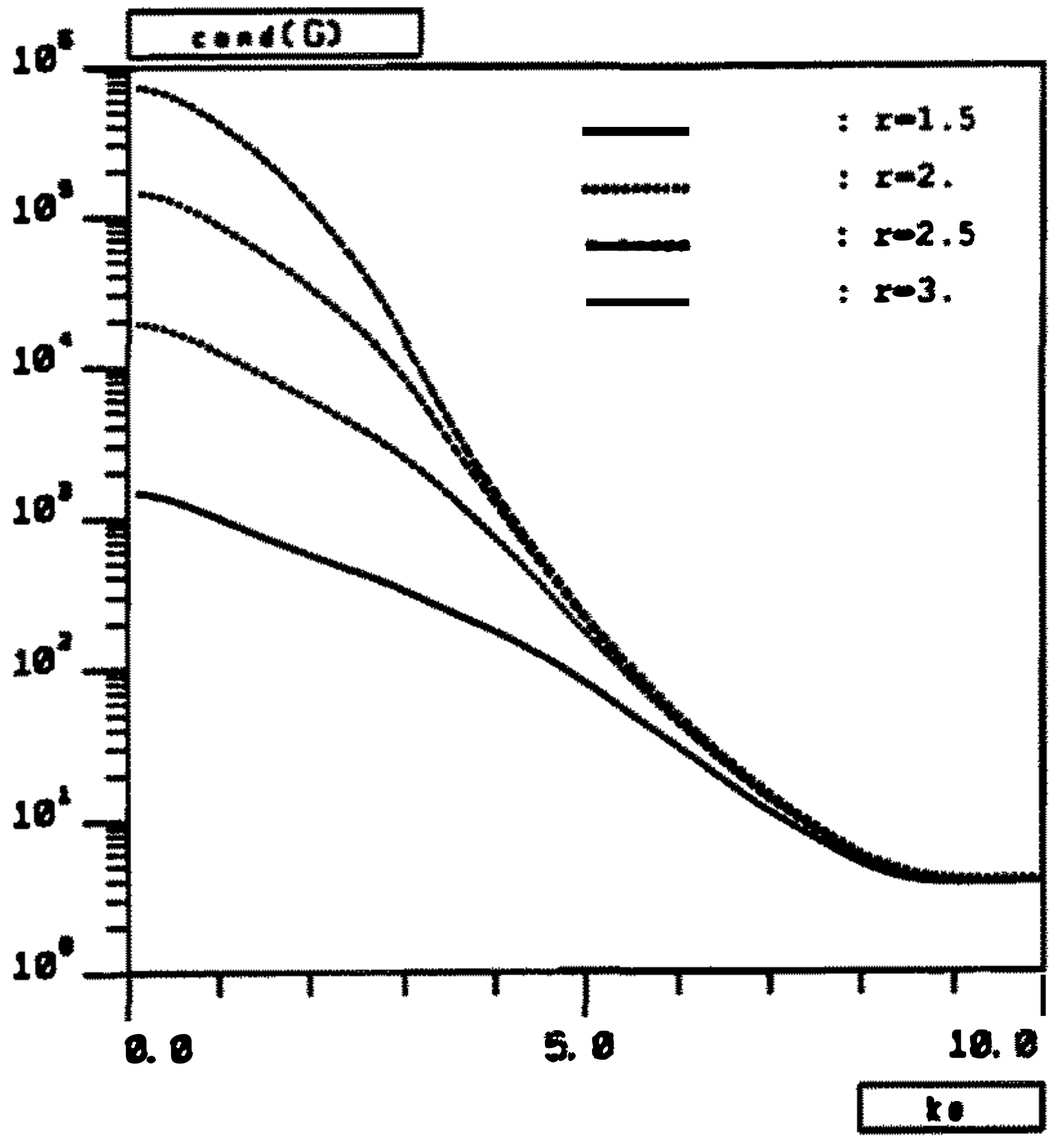

Fig. 5. — Cond(**G**) against ka, for several values of r.

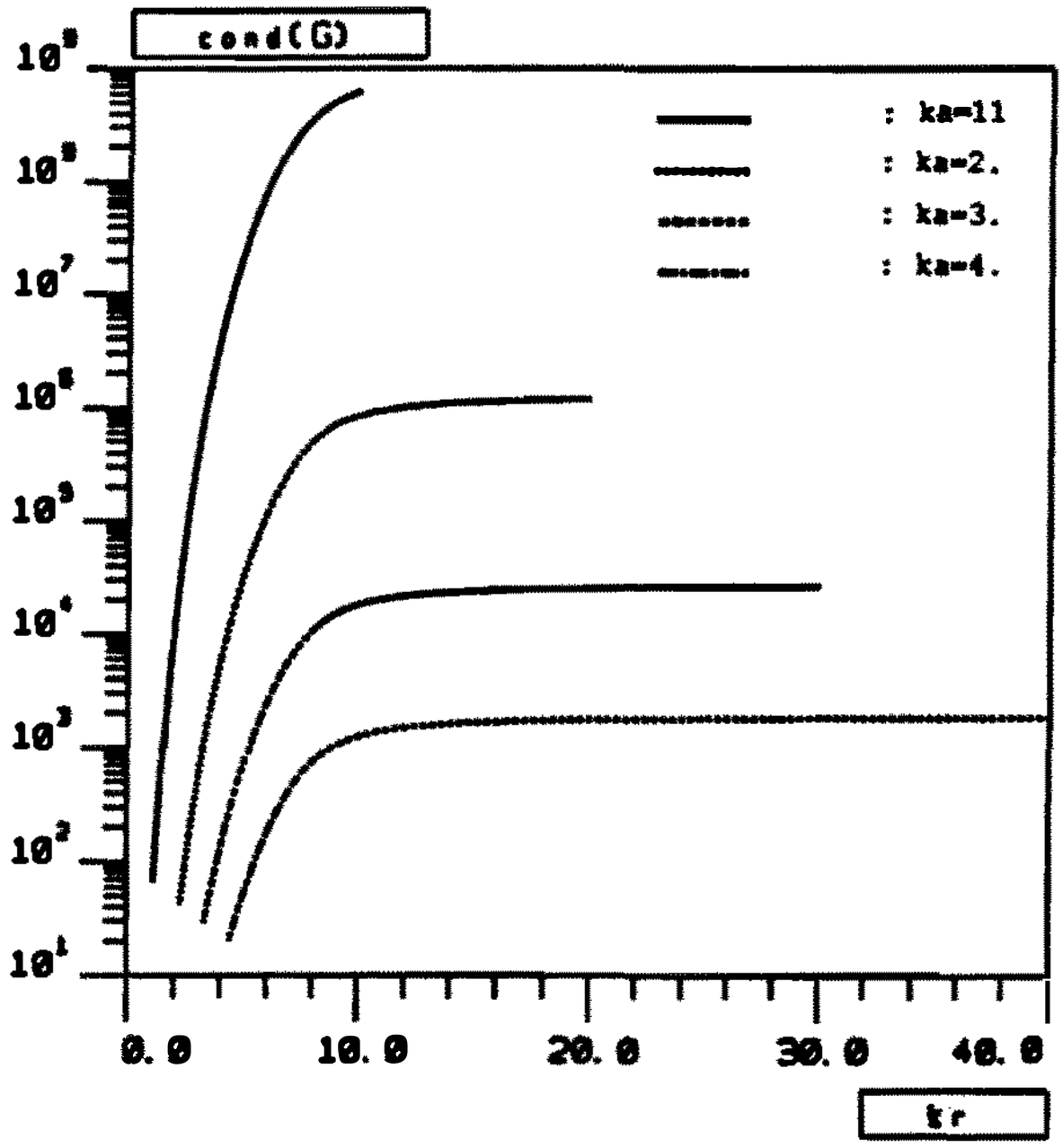

Fig. 6. — Cond(**G**) against kr, for several values of ka.

integration point $\mathbf{y} = (y_1, y_2, y_3)$ in equation (1.6) is directed towards the interior of S. As a first step, solving the integral equation (1.6) allows the determination of the pressure field p on S given U (Neumann boundary value problem). Then the value $p(\mathbf{x})$ of the pressure field is known, for every $\mathbf{x}$ outside S, using the well-known integral representation:

$$p(\mathbf{x}) = -\frac{i}{\rho\omega}\int_S U(\mathbf{y})G(\mathbf{x},\mathbf{y})\,\mathrm{d}S_\mathbf{y} - \int_S p(\mathbf{y})n_s(\mathbf{y})\frac{\partial}{\partial y_s}G(\mathbf{x},\mathbf{y})\,\mathrm{d}S_\mathbf{y} \qquad (1.7)$$

Equations (1.6, 1.7) give an integral equation formulation of the direct Neumann acoustical problem. The inverse problem we are interested in is: given measured values of the pressure field p radiated in the free-space outside the vibrating surface S, find the distribution of normal velovity U on S.

It is apparent that the representation (1.7) does not yield the direct linear operator G, such that $\mathbf{G}U = p$, relating p in the free space to U on S: in fact (1.7) involves the values on S of the pressure field, which are known through the integral equation (1.6). thus let us write formally equations (1.6) and (1.7) as follows (P denoting the discrete set of the measured values of p):

$$\mathbf{K}p + \mathbf{L}U = 0 \qquad \text{and} \quad \mathbf{K}_1 p + \mathbf{L}_1 U = \mathrm{P} \qquad (1.6b\text{-}1.7b)$$

we get:

$$\left[-\mathbf{K}_1\mathbf{K}^{-1}\mathbf{L} + \mathbf{L}_1\right] U = P \qquad (1.8)$$

and equation (1.8) gives formally the linear operator G for the direct problem:

$$\mathbf{G} = -\mathbf{K}_1\mathbf{K}^{-1}\mathbf{L} + \mathbf{L}_1 \qquad (1.9)$$

Now let us assume that a boundary element discretization process has been performed, in a standard fashion [16, 17], on the surface S and the surface fields p, U, the discrete counterpart of the unknown U being a set of n nodal values $U_1, \ldots, U_n$. The integral equation (1.6) written for a finite number n_c of *collocation points* $\mathbf{x} = \mathbf{x}_1, \ldots \mathbf{x}_{n_c}$ (which are often chosen as the n nodes which define the boundary element interpolation of U, in which case $n_c = n$) and the integral representation (1.7) written for the pressures $p(\mathbf{X}_1), \ldots p(\mathbf{X}_m)$ at the m measurement points $\mathbf{x} = \mathbf{X}_1, \ldots \mathbf{X}_m$ lead to (1.6b-1.7b), understood as algebraic relations, in which the operators K, L are complex matrices (fully populated and nonsymmetric) of size $n \times n$ and $\mathbf{K}_1$, $\mathbf{L}_1$ complex matrices of size $m \times n$.

The discrete problem consists here in searching for the modal values $U_1, \ldots U_n$ of the normal velocity using the linear relation:

$$\mathbf{GU} \equiv \left(-\mathbf{K}_1\mathbf{K}^{-1}\mathbf{L} + \mathbf{L}_1\right)\mathbf{U} = \mathbf{P} \qquad \text{with} \qquad \mathbf{U} = [U_1, \ldots, U_n]\,,\ \mathbf{P} = [p(\mathbf{X}_1), \ldots p(\mathbf{X}_m)] \qquad (1.10)$$

2. Gaussian inversion for a linear inverse problem.

The inverse problem stated in section 1.2 is linear. It is well known [18-11] that the actual solution of inverse problems is generally highly sensitive to measurement and/or modelling errors, due to their ill-posedness: the solution of an inverse problem is generally not continuous with respect to the measurements. Several approaches aim to replace the exact solution, if any, by defining an approximate solution; their purpose is to restore the continuity of the inversion process with respect to the data by relaxing the concept of solution in an appropriate way and using stabilization

methods of various types. Among these approaches are the Tikhonov regularization [21], the stochastic inversion [10], the quasi-reversibility method [22]. These approaches rely in fact on similar basic concepts: modelling of measurement errors, use of *a priori* extra informations to stabilize the inversion process with respect to the data; they lead to similar optimization problems for the actual solution of a given inverse problem and the differences between them appear mostly, in our opinion, in the interpretation attached to the quantities and operators involved in each particular strategy.

Having highlighted in section 1.1 above the ill-conditioned character of the present inverse problem, we will focus on the use of one of these approaches, namely the stochastic inversion, and more specifically the Gaussian inversion method [10]. Our choice is motivated by two reasons: firstly the improved stability of the inversion result with respect to data fluctuations, secondly the ability of this method to give easily interpretable confidence indicators, as it will be seen in the subsequent developments. Besides, other probability laws may be used instead of the Gaussian one for defining a stochastic interpretation of an inverse problem, but the Gaussian modelling is the only one leading to a linear inversion procedure (of the linear least-squares type) if the physical model itself is linear. It is to be noticed that the authors of [2, 3] use a *truncated* singular value decomposition to solve numerically their linear least-squares problem. This truncation has a stabilizing effect by eliminating the magnification of the data noise caused by the smallest singular values; it is indeed a particular case of Tikhonov regularization. However the guidelines for choosing the adequate truncation level, as well as the behaviour of the (truncated) singular value decomposition, seem to be unclear. The present approach combines the simplicity of more usual least squares methods, such as the Householder decomposition, with stabilizing properties and access to confidence or dispersion estimators.

2.1 BASIC DEFINITIONS AND RESULTS [10]. — Let us consider two spaces M (parameter space) and D (data space), being respectively associated here to the normal velocities on S and the measured pressure values. The direct problem under consideration is modelled using a linear operator $G: M \to D$ (defined by equation (1.10) in our particular case). The corresponding inverse problem is stated as:

$$\text{Find } \mathbf{m} \in M \text{ such that } \mathbf{G}\mathbf{m} = \mathbf{d}_{obs} \quad (\text{given } \mathbf{d}_{obs} \in D) \tag{2.1}$$

The spaces D and M have finite dimensions m and n respectively (the inverse problem being discretized): $M = \mathbb{R}^n$ or $\mathbb{C}^n$ and $D = \mathbb{R}^m$ or $\mathbb{C}^m$.

In the Gaussian inversion approach, the vectors $\mathbf{m}$ and $\mathbf{d}_{obs}$ are viewed as multidimensional Gaussian random variables, in order to model noisy data $\mathbf{d}_{obs}$ and subsequent uncertainties on the result $\mathbf{m}$. We know from the classical probability theory that a Gaussian random N-dimensional variable $\mathbf{y} = [y_j]_{j=1,N}$ (each y_j being a scalar random variable) is characterized by the data of its *mean* (or *mathematical expectation*) $\langle \mathbf{y} \rangle$ and its (positive definite) *covariance matrix* $\mathbf{C}$; such a variable will be symbolically noted $\mathbf{y} = N(\langle \mathbf{y} \rangle, \mathbf{C})$. Its probability density f is equal to:

$$f(\mathbf{y}) = [(2\pi)^N \det(\mathbf{C})]^{-1/2} \exp\left(-\frac{1}{2}(\mathbf{y} - \langle \mathbf{y} \rangle)^* \mathbf{C}^{-1} \langle \mathbf{y} - \langle \mathbf{y} \rangle \rangle\right) \tag{2.2}$$

The data required by the Gaussian inversion approach, are in addition of G and $\mathbf{d}_{obs}$ which are obviously necessary for any inversion procedure to give results:

(a) A Gaussian probability law $N(\mathbf{d}_{obs}, \mathbf{C}_D)$ describing the information available about the quality of the data $\mathbf{d}_{obs}$.

(b) A Gaussian probability law $N(\mathbf{m}_{prior}, \mathbf{C}_M)$ describing *a priori* information about $\mathbf{m}$.

The a priori information is generally some knowledge of $\mathbf{m}$ coming from general physical considerations. In the Gaussian framework one assumes *a priori* that $\mathbf{m}_{prior}$ is an acceptable reference

value for $\mathbf{m}$, the covariance matrix $\mathbf{C_M}$ defining "soft bounds": the smaller $\mathbf{C_M}$, the more accurate *a priori* information.

Thus one possesses two *independent* informations about $\mathbf{m}$: the *a priori* information and the fact that $\mathbf{m}$ and the measurements $\mathbf{d_{obs}}$ are related by the *physical model* G. The *conjunction* of these informations on $\mathbf{m}$ leads to the statement that $\mathbf{m}$ follows in fact an *a posteriori* Gaussian probability law $N(\langle \mathbf{m} \rangle, \mathbf{C})$, which covariance operator $\mathbf{C}$ and mean $\langle \mathbf{m} \rangle$ result from the minimization with respect to $\mathbf{m}$ of:

$$2S(\mathbf{m}) = (\mathbf{G}(\mathbf{m}) - \mathbf{d_{obs}})^* \, \mathbf{C_D^{-1}} \, (\mathbf{G}(\mathbf{m}) - \mathbf{d_{obs}}) + (\mathbf{m} - \mathbf{m_{prior}})^* \, \mathbf{C_M^{-1}} \, (\mathbf{m} - \mathbf{m_{prior}}) \qquad (2.3)$$

and are equal to:

$$\mathbf{C} = \left[\mathbf{G}^* \, \mathbf{C_D^{-1}} \, \mathbf{C} + \mathbf{C_M^{-1}}\right]^{-1} \qquad \langle \mathbf{m} \rangle = \mathbf{C} \left[\mathbf{G}^* \, \mathbf{C_D^{-1}} \, \mathbf{d_{obs}} + \mathbf{C_M^{-1}} \, \mathbf{m_{prior}}\right] \qquad (2.4)$$

Tarantola gives other interesting expressions for $\langle \mathbf{m} \rangle$ and $\mathbf{C}^{-1}$ equivalent to (2.4); the following ones, which, unlike (2.4), do not require the inverses of the covariance operators, will prove useful:

$$\mathbf{C} = \mathbf{C_M} - \mathbf{C_M} \, \mathbf{G}^* \, [\mathbf{G} \, \mathbf{C_M} \, \mathbf{G}^* + \mathbf{C_D}]^{-1} \, \mathbf{G} \, \mathbf{C_M} \qquad (2.5a)$$

$$\langle \mathbf{m} \rangle = \mathbf{m_{prior}} + \mathbf{C_M} \, \mathbf{G}^* \, [\mathbf{G} \, \mathbf{C_M} \, \mathbf{G}^* + \mathbf{C_D}]^{-1} \, [\mathbf{d_{obs}} - \mathbf{G m_{prior}}] \qquad (2.5b)$$

The results of the Gaussian inversion method are the *a posteriori* mean $\langle \mathbf{m} \rangle$ and covariance $\mathbf{C}$. Using these quantities one can define as follows *confidence indicators* associated to the solution $\langle \mathbf{m} \rangle$.

2.2 Definitions of a posteriori confidence indicators.

2.2.1 *A posteriori covariances and "error ellipsoïd".* — The ellipsoïd (in the n-dimensional space M) defined by:

$$2S(\mathbf{m}) = \mathbf{m}^* \mathbf{C}^{-1} \mathbf{m} = 1 \qquad (2.6)$$

is geometrically representative of the dispersion of the *a posteriori* distribution over $\mathbf{m}$. Its principal axes are the *a posteriori* principal standard deviations σ_i^{post}, that is, the positive square roots of the eigenvalues C_i of $\mathbf{C}$; the geometrical mean $\langle \sigma^{\text{post}} \rangle$ of the principal standard deviations σ_i^{post} is given by:

$$\langle \sigma^{\text{post}} \rangle = [\det(\mathbf{C})]^{1/2n} \qquad (2.7)$$

The consideration of $\langle \sigma^{\text{post}} \rangle$ gives a global idea of the overall quality of the inversion, which is not always tha case when considering the diagonal terms C_{ii} of $\mathbf{C}$ (variances associated to $\langle \mathbf{m} \rangle_i$), especially when $\mathbf{C}$ exhibits strong correlations between the $\langle \mathbf{m} \rangle_i$.

On can also consider the ratio of the volumes of the *a posteriori* and *a priori* error ellipsoïds, defined as:

$$\frac{V}{V_{\mathbf{M}}} = \frac{[\det(\mathbf{C})]^{1/2}}{[\det(\mathbf{C_M})]^{1/2}} = \frac{\langle \sigma^{\text{post}} \rangle^n}{\langle \sigma^{\text{prior}} \rangle^n} \qquad (2.8)$$

which gives a measure of the information gained between the *a priori* and *a posteriori* state.

2.2.2 *Relative information.* — Another interesting indicator, provided by the information theory, is the relative information content of a probability density f_1 with respect to another probability density f_0, defined as:

$$\mathrm{IR}(f_1, f_0) = \int f_1(\mathbf{x}) \log \frac{f_1(\mathbf{x})}{f_0(\mathbf{x})} \, \mathrm{d}\mathbf{x} \tag{2.9}$$

One can apply definition (2.9) to the particular case $f_0 = \mu$ (μ being the null information probability density); then $\mathrm{IR}(f_1; \mu)$ is the *information content* of f_1. Furthermore $\mathrm{IR}(f_1; f_0)$ being nonnegative means that $f_1(\mathbf{x})$ contains more information about $\mathbf{x}$ than $f_0(\mathbf{x})$.

If both f_1 and f_0 are Gaussian probability densities, the algebraic expression of $\mathrm{IR}(f_1; f_0)$ is known [10]. In particular if f_0 and f_1 are respectively the *a priori* and *a posteriori* probability densities involved in the linear gaussian inversion process, $\mathrm{IR}(f_1; f_0)$ (which in this case will be denoted simply IR) is given by:

$$2\mathrm{IR} = [\langle \mathbf{m} \rangle - \mathbf{m}_{\mathrm{prior}}]^* \, \mathbf{C}_{\mathbf{M}}^{-1} \, [\langle \mathbf{m} \rangle - \mathbf{m}_{\mathrm{prior}}] - \mathrm{Log} \frac{\det(\mathbf{C})}{\det(\mathbf{C})_{\mathbf{M}}} + \mathrm{Tr}\left[\mathbf{C}_{\mathbf{M}} \mathbf{C}^{-1} - \mathbf{I}\right] \tag{2.10}$$

It is apparent that in the limiting case $\mathbf{C} = \epsilon \mathbf{C}_{\mathbf{M}}$ (ϵ small), that is, in the case of an *a posteriori* uncertainty much smaller than the *a priori* one, IR behaves asymptotically like $1/\epsilon$ and can therefore take arbitrarily large values. In the opposite case where $(\langle \mathbf{m} \rangle, \mathbf{C})$ are equal to $(\mathbf{m}_{\mathrm{prior}}, \mathbf{C}_{\mathbf{M}})$, which means that the result of the Gaussian inversion is equal to the *a priori* knowledge, IR vanishes as expected.

2.2.3 *Resolution operator.* — Assume that there exists $\mathbf{m}_{\mathrm{exact}}$ such that:

$$\mathbf{G}\mathbf{m}_{\mathrm{exact}} = \mathbf{d}_{\mathrm{obs}} \tag{2.11}$$

The resolution operator $\mathbf{R}$ appears [14], [1]when one expresses $\langle \mathbf{m} \rangle$ in terms of $\mathbf{m}_{\mathrm{exact}}$:

$$\langle \mathbf{m} \rangle = \left[\mathbf{I} - \mathbf{C}\mathbf{C}_{\mathbf{M}}^{-1}\right] \mathbf{m}_{\mathrm{exact}} + \mathbf{C}\mathbf{C}_{\mathbf{M}}^{-1} \, \mathbf{m}_{\mathrm{prior}} = \mathbf{R}\mathbf{m}_{\mathrm{exact}} + \mathbf{C}\mathbf{C}_{\mathbf{M}}^{-1} \, \mathbf{m}_{\mathrm{prior}} \tag{2.12}$$

Equation (2.12) shows that the smaller (in matrix norm sense) the *a posteriori* covariance matrix $\mathbf{C}$ compared to $\mathbf{C}_{\mathbf{M}}$, the better the solution $\langle \mathbf{m} \rangle$. In other words, a good Gaussian inversion coincides with a matrix $\mathbf{C}\mathbf{C}_{\mathbf{M}}^{-1}$ small compared to I. All the eigenvalues of the matrix $\mathbf{C}\mathbf{C}_{\mathbf{M}}^{-1}$, which is positive definite, are real and positive, its trace is also positive. Thus one always has:

$$\mathrm{Tr}\left[\mathbf{I} - \mathbf{C}\mathbf{C}_{\mathbf{M}}^{-1}\right] \leq \mathrm{Tr}(\mathbf{I}) \tag{2.13}$$

or

$$r := \frac{\mathrm{Tr}\left[\mathbf{I} - \mathbf{C}\mathbf{C}_{\mathbf{M}}^{-1}\right]}{\mathrm{Tr}(\mathbf{I})} \leq 1 \tag{2.14}$$

The number $r \leq 1$ (2.14) characterizes the resolution quality, it should be the nearest possible from unity ($r = 1$ corresponds to a perfect resolution).

2.3 INTERPRETATION OF COVARIANCE OPERATORS ASSOCIATED TO COMPLEX-VALUED GAUSSIAN RANDOM VARIABLES. — Acoustical problems frequently involve complex-valued variables (pressure, velocity, velocity potential, ...). For the present problem, G is a linear operator which relates the complex-valued pressure field in the free space to the complex-valued field of normal velocity on the vibrating surface. The infinite-dimensional version of G is defined using integral operators with complex-valued kernels, while after discretization G will be a matrix with complex-valued coefficients.

Obviously one can split each complex number into its real and imaginary parts, obtaining an equivalent problem with real-valued variables. However, using such a transformation, the computation done in real arithmetic needs twice the storage and the computer time required for the same computation done in complex arithmetic.

Thus it seems desirable to work within the usual complex arithmetic framework. More precisely, we wish to apply formulae (2.3) or (2.5) expressing the gaussian inversion result to *complex-valued* Gaussian random variables. In this case, one has to give some sense to formulae like (2.3), and particularly to *complex* covariance matrices.

We are then led to consider expressions such as:

$$s(\mathbf{m}) = \mathbf{m}^* \mathbf{A} \mathbf{m} \tag{2.15}$$

where $\mathbf{m}$ is a complex vector and $\mathbf{A}$ a complex hermitian positive definite matrix. Let us split (2.15) into real and imaginary parts; taking into account the hermitian character of $\mathbf{A}$, we can write:

$$\mathbf{A} = \mathbf{A}_R + i\mathbf{A}_I \quad \text{with} \quad (\mathbf{A}_R)^t = \mathbf{A}_R \quad \text{and} \quad (\mathbf{A}_I)^t = -\mathbf{A}_I \; ; \qquad \mathbf{m} = \mathbf{x} + i\mathbf{y} \tag{2.16}$$

and then

$$s(\mathbf{m}) = s(\mathbf{x} + i\mathbf{y}) = [\mathbf{x}\ \mathbf{y}] \begin{bmatrix} \mathbf{A}_R & -\mathbf{A}_I \\ -\mathbf{A}_I & \mathbf{A}_R \end{bmatrix} \begin{bmatrix} \mathbf{x} \\ \mathbf{y} \end{bmatrix} \tag{2.17}$$

In the decomposition (2.17), the positive definiteness of the bilinear form $s(\mathbf{m})$ implies the inversibility of the matrix $\mathbf{A}_R$ (write (2.17) with $\mathbf{x} = 0$ or $\mathbf{y} = 0$).

Going back to the covariance matrice C, C appears as the inverse of A in the quadratic forms like (2.15) involved in the définition (2.2) of a random Gaussian vector. Thus let us examine the inverse of the matrix appearing in the decomposition (2.17) of $s(\mathbf{m})$, this inverse being the real-variable substitute for the complex covariance matrix C. An algebraic manipulation shows that:

$$\begin{bmatrix} \mathbf{A}_R & -\mathbf{A}_I \\ \mathbf{A}_I & \mathbf{A}_R \end{bmatrix}^{-1} = \begin{bmatrix} \left[\mathbf{A}_R + \mathbf{A}_I (\mathbf{A}_R)^{-1} \mathbf{A}_I\right]^{-1} & -(\mathbf{A}_R)^{-1} \mathbf{A}_I \left[\mathbf{A}_R + \mathbf{A}_I (\mathbf{A}_R)^{-1} \mathbf{A}_I\right]^{-1} \\ (\mathbf{A}_R)^{-1} \mathbf{A}_I \left[\mathbf{A}_R + \mathbf{A}_I (\mathbf{A}_R)^{-1} \mathbf{A}_I\right]^{-1} & \left[\mathbf{A}_R + \mathbf{A}_I (\mathbf{A}_R)^{-1} \mathbf{A}_I\right]^{-1} \end{bmatrix} \tag{2.18}$$

the diagonal blocks of the matrix (2.18) being symmetric while the non-diagonal ones are anti-symmetric.

This result remains to be interpreted in terms of covariances. The examination of equation (2.18) shows that, in the framework of a Gaussian random variable modelling, the component C_{ij} of the *complex* matrix C, which relates the *complex* components m_i and m_j of $\mathbf{m}$, can be interpreted as follows:

• Re (C_{ij}) is the *common* value of the covariance coefficients between the two real parts x_i, x_j on one hand, between the two imaginary parts y_i, y_j on the other hand. In other words, the complex variable modelling assumes for every pair (m_i, m_j) the correlations between the real parts and between the imaginary parts to be equal.

• Im (C_{ij}) is the *common* value of the covariance coefficients between y_i, x_j and between x_i, y_j. In other words, the complex variable modelling assumes for every pair (m_i, m_j) the correlations between x_i, y_j on one hand, and between y_i, x_j on the other hand, to be of equal absolute values and opposite signs. For the particular case $i = j$, these correlations vanish: the use of complex number representation implies that the real and imaginary parts of any complex component m_i are independent in probability.

Therefore it is possible to perform a Gaussian inversion using complex arithmetics, if one keeps in mind the above-mentioned meaning and limitations implied on the covariance terms. Equations (2.2) to (2.9) and (2.11) to (2.14), originally written for real-variable problems, remain valid for complex parameter and data spaces, the star denoting hemitian transposition (i.e. transposition and conjugation) instead of mere transposition. On the contrary, the expression (2.10), as stated, is only valid for *real-valued* Gaussian random variables. One can extend it to complex-valued variables by rewriting (2.10) in terms of real coefficients using (2.16), (2.17) and (2.18) and calculate IR using the real covariance matrix associated to $\mathbf{C_M}$. Then the complex variable expression of IR becomes:

$$2\mathrm{IR} = \left[\langle \mathbf{m} \rangle - \mathbf{m}_{\mathrm{prior}}\right]^{*} \mathbf{C}_{\mathbf{M}}^{-1} \left[\langle \mathbf{m} \rangle - \mathbf{m}_{\mathrm{prior}}\right] - 2\,\mathrm{Log}\frac{\det(\mathbf{C})}{\det(\mathbf{C_M})} + 2\mathrm{Tr}\left[\mathbf{C}\mathbf{C}_{\mathbf{M}}^{-1} - \mathbf{I}\right] \qquad (2.19)$$

2.4 INVERSION ALGORITHM AND INTERPRETATION OF THE RESULTS. — The operator $\mathbf{G}$ is expressed as a matrix $m \times n$ with complex coefficients; the matrix $n \times m$ of the adjoint operator $\mathbf{G}^*$ being obtained by conjugating and transposing $\mathbf{G}$: $g^*_{ij} = \overline{g_{ji}}$.

Let us recall that, from the very definition of covariance operator, the (*a priori* and *a posteriori*) covariance matrices are symmetric and positive definite; thus they can be factored using the Choleski decomposition:

$$\mathbf{C_M} = \mathbf{C}_{\mathbf{M}}^{*/2}\mathbf{C}_{\mathbf{M}}^{1/2} \qquad \mathbf{C_D} = \mathbf{C}_{\mathbf{D}}^{*/2}\mathbf{C}_{\mathbf{D}}^{1/2} \qquad \mathbf{C} = \mathbf{C}^{*/2}\mathbf{C}^{1/2} \qquad (2.20)$$

2.4.1 *"One-by-one" inversion of the data.* — In practical studies one has often to assume the measurement errors to be statistically independent, this is equivalent to assume the matrix $\mathbf{C_D}$ to be diagonal:

$$\mathbf{C_D} = \mathrm{diag}\left[(\sigma^1)^2, (\sigma^2)^2, \ldots, (\sigma^m)^2\right] \qquad (2.21)$$

In this case it is possible to define an inversion procedure which treats the data values *one-by-one*. It will rely on the use of (2.5a-b), which is valid whatever the number m of data values, even $m = 1$. In this purpose, let us denote by $\{\langle \mathbf{m} \rangle_p, \mathbf{C}_p\}$ the result obtained by Gaussian inversion of the first p data values, $\{\langle \mathbf{m} \rangle^0, \mathbf{C}^0\}$ denoting the *a priori* quantities $\{\mathbf{m}_{\mathrm{prior}}, \mathbf{C_M}\}$. The p-th row of $\mathbf{G}$ and the p-th data value will be respectively denoted by $\mathbf{g}_p$ and d_p^{obs}. Inversion of datum d_p^{obs} with *a priori* data $\langle \mathbf{m} \rangle_{p-1}$, $\mathbf{C}_{p-1}$ leads to the same result as the inversion of the first p data values with *a priori* data $\mathbf{m}_{\mathrm{prior}}$ and $\mathbf{C_M}$[1].

Inversion of d_p^{obs} using (2.5a-b) leads to the following relation between $\mathbf{C}_p$ and $\mathbf{C}_{p-1}$:

$$\mathbf{C}_p = \mathbf{C}_{p-1}^{*/2}\left[\mathbf{I} - \alpha_p \mathbf{v}_{p-1}\mathbf{v}_{p-1}^{*}\right]\mathbf{C}_{p-1}^{1/2} \qquad \text{with } \mathbf{v}_p = \frac{1}{\sigma_p}\mathbf{C}_{p-1}^{1/2}\mathbf{g}^p; \quad \alpha_p = \sigma_p^2\beta_p = \frac{1}{\mathbf{v}_p^{*}\mathbf{v}_p + 1} \qquad (2.22)$$

the corresponding relation between $\mathbf{m}_p$ and $\mathbf{m}_{p-1}$, obtained using (2.5b), being:

$$\mathbf{m}_p = \mathbf{m}_{p-1} + \frac{1}{\sigma_p}\alpha_p \mathbf{C}_{p-1}^{*/2}\mathbf{v}_p\left[d_p^{\mathrm{obs}} - \mathbf{g}_p\mathbf{m}_{p-1}\right] \qquad (2.23)$$

Equations (2.22) and (2.23) define the p-th step step of a "one-by-one" version of the Gaussian inversion method. This procedure does not require the inversion of a matrix (the inverse matrix in (2.5) degenerating into the scalar $1/\beta_p$). On the other hand, the updating of $\mathbf{C}_p$ using equation (2.22) seems costly at first sight, requiring two matrix-vector and one matrix-matrix products at each step. In fact it is possible to perform (2.22) in a cheaper way, taking into account the particular structure of the transfer relation (2.22) between $\mathbf{C}_{p-1}$ and $\mathbf{C}_p$. This relies upon the fact that an exact expression of the Choleski decomposition of a matrix $\mathbf{T}$ of the form: $\mathbf{T}=\mathbf{I}-\alpha\mathbf{v}\mathbf{v}^*$ with $\alpha\mathbf{v}^*\mathbf{v}<1$ (such a matrix is positive definite) is known:

$$\mathbf{T}=\mathbf{T}^{*1/2}\mathbf{T}^{1/2} \quad \text{with} \quad \left(\mathbf{T}^{1/2}\right)_{ii}=\left(\frac{1-\alpha s_i}{1-\alpha s_{i-1}}\right)^{1/2};\ \left(\mathbf{T}^{1/2}\right)_{ij}=\frac{-\alpha v_i \bar{v}_j}{((1-\alpha s_i)(1-\alpha s_{i-1}))^{1/2}} \tag{2.24a}$$

$$s_i=v_1^* v_1+\ldots+v_i^* v_i \tag{2.24b}$$

Upon application of this result to the matrix $\mathbf{T}_p=\mathbf{I}-\alpha_p\mathbf{v}_p\mathbf{v}_p^*$, the transferrelation between $\mathbf{C}_{p-1}^{1/2}$ and $\mathbf{C}_p^{1/2}$ is known:

$$\mathbf{C}_p^{1/2}=\mathbf{T}_p^{1/2}\mathbf{C}_{p-1}^{1/2} \tag{2.25}$$

$\mathbf{T}_p$ being defined by (2.24a-b). By applying the same method during the inversion of each individual datum, we get:

$$\mathbf{C}^{1/2}=\mathbf{C}_m^{1/2}=\mathbf{K}\mathbf{C}_{\mathrm{M}}^{1/2} \qquad \text{with} \quad \mathbf{K}=\mathbf{T}_m^{1/2}\ldots\mathbf{T}_2^{1/2}\mathbf{T}_1^{1/2} \tag{2.26}$$

In fact all the *a posteriori* interpretations, including the computation of the indicators introduced in section 2.2, can be made using only $\mathbf{C}^{1/2}$; the actual computation of $\mathbf{C}$ is unnecessary for our purposes and will therefore be omitted.

Finally let us remark that the matrix $\mathbf{v}\mathbf{v}^*$ has rank one; it admits the eigenvalue 0 associated to the eigenvector $\mathbf{v}$ with multiplicity $(n-1)$ and the eigenvalue $\mathbf{v}^*\mathbf{v}$ with multiplicity 1. Then:

$$\det(\mathbf{v}\mathbf{v}^*)=0 \qquad \det(\mathbf{I}-\alpha\mathbf{v}\mathbf{v}^*)=1-\alpha\mathbf{v}^0\mathbf{v}=\alpha \tag{2.27}$$

which implies:

$$\det\left(\mathbf{C}_p^{1/2}\right)=\alpha_p^{1/2}\det\left(\mathbf{C}_{p-1}^{1/2}\right) \tag{2.28}$$

2.4.2 *Evaluation of step by step indicators.* — We give the algebraic expressions of the indicators introduced in section 2.2 associated to the inversion of the p-th datum, the $(p-1)$ state being accordingly considered as the *a priori* state for this step. Using (2.28), one has immediately:

$$\frac{V}{V_{\mathrm{M}}}=(\alpha_p)^{n/2} \qquad \text{and} \qquad \frac{\langle\sigma^{\mathrm{post}}\rangle}{\langle\sigma^{\mathrm{prior}}\rangle}=\sqrt{\alpha_p} \tag{2.29}$$

Besides, it is easy to obtain the following expression for IR at step p using (2.23) and (2.27):

$$2\mathrm{IR}=\alpha_p\mathbf{v}_p^*\mathbf{v}_p\left[\frac{1}{\sigma_p^2}\alpha_p\left(d_p^{\mathrm{obs}}-\mathbf{g}_p\mathbf{m}_{p-1}\right)^2-2\right]-2\mathrm{Log}\,\alpha_p \tag{2.30}$$

The evaluation of quantities (2.29) and (2.30) after inversion of each datum re-uses quantities already computed during the inversion process, thus needing very few extra computer time. It allows one to check the overall inversion procedure and gives some indication about the information content brought by each individual datum.

2.4.3 *Evaluation of global inversion indicators.* — The interpretation, in terms of confidence or quality, of the final result obtained by Gaussian inversion uses the values of the global (i.e. after inversion of the m data values) indicators. These ones can be expressed in terms of the scalars α_p and the matrix $\mathbf{K}$ defined by (2.26b):

$$\frac{\Delta V}{V} = \frac{[\det(\mathbf{C})]^{1/2}}{[\det(\mathbf{C}_M)]^{1/2}} = [\det(\mathbf{K})]^{1/2} = (\alpha_1 \ldots \alpha_m)^{1/2} \qquad \text{and} \qquad \frac{\left\langle \sigma_i^{\text{post}} \right\rangle}{\left\langle \sigma_i^{\text{prior}} \right\rangle} = (\alpha_1 \ldots \alpha_m)^{n/2} \tag{2.31-2.32}$$

On the other hand:

$$\text{Tr}\left[\mathbf{C}_M \mathbf{C}^{-1} - \mathbf{I}\right] = \text{Tr}\left[\mathbf{K}^* \mathbf{K} - \mathbf{I}\right] = -n + \sum_{(i,j),\, i \leq j} |K_{ij}|^2 \tag{2.33}$$

The relative information between the *a posteriori* and *a priori* states for the global inversion, is then equal to :

$$2\text{IR} = \left[\langle \mathbf{m} \rangle - \mathbf{m}_{\text{prior}}\right]^* \mathbf{C}_M^{-1} \left[\langle \mathbf{m} \rangle - \mathbf{m}_{\text{prior}}\right] - 2 \left[\sum_{1 \leq i \leq m} \text{Log}\, \alpha_i \right] - 2n + 2 \left[\sum_{(i,j),\, i \leq j} |K_{ij}|^2 \right] \tag{2.34}$$

Finally the coefficient r characterizing the resolution quality, defined by (2.14), is in this case equal to:

$$r = 1 - \frac{1}{n} \left[\sum_{(i,j),\, i \leq j} |K_{ij}|^2 \right] \tag{2.35}$$

2.5 A POSTERIORI EXAMINATION OF THE GAUSSIAN ASSUMPTION AND DETECTION OF OUTLIERS. — This part presents, as a complement for the numerical implementation of the Gaussian inversion, a method for the detection of outliers, i.e. the data values which are highly erroneous compared to the standard deviations of measurement errors given the covariance matrix $\mathbf{C}_D$. The solution $\langle \mathbf{m} \rangle$ of the Gaussian inversion is, as seen in (2.1), a minimizer of the least-squares type functional $S\langle \mathbf{m} \rangle$, given by (2.3).

It is shown [1] that the random variable defined as the minimum value of the functional $2S(\mathbf{m})$ follows a χ^2 *distribution*, with $2m$ or m degrees of freedom for complex-variable or real-variable problems respectively (m being the dimension of the data space D). $\chi^2(m)$ is the well-known statistical law associated to the sum of the squares of m Gaussian scalar real-valued random variables of zero mean and unit standard deviation.

This result is interesting as it allows an *a posteriori* check of the Gaussian assumption which has been made for all the quantities involved in the inverse problem. This check is made by evaluating the probability:

$$P = P\left(\chi^2(2m) \leq 2S(\langle \mathbf{m} \rangle)\right) \tag{2.36}$$

in which we consider a complex-variable inverse problem. The expression $f\left(\chi^2(\nu)\right)$ of the probability density associated to the $\chi^2(\nu)$ law is well known. In our gaussian inversion computer code, this probability is computed using the function GAMMP, from the software library "Numerical Recipes" [24]:

$$P\left(\chi^2(2m) \leq 2S(\langle \mathbf{m} \rangle)\right) = \text{GAMMP}(m,\, S(\langle \mathbf{m} \rangle)) \tag{2.37}$$

Once the value of P is computed, three cases can occur:

(i) P is neither very small (near zero), nor very large (near unity). In this case the Gaussian assumption remains plausible, although this result can by no means be considered as a definite confirmation.

(ii) P is very small. In this case the gaussian assumption itself is not in doubt; nevertheless it is likely that the estimated error for the data values have been postulated in a "conservative" way; in other words the data errors are smaller than expected.

(iii) P is very close to unity. In this case the Gaussian assumption is highly questionable. This is often associated to the presence of a small (compared to the size m of the data set) number of outliers in the data $\mathbf{d}^{\mathbf{obs}}$. Typically "very close to unity" means "greater or equal than 0.99 (for even 0.999)" [24]. In practice, outliers often create on the value $S(\langle \mathbf{m} \rangle)$ distortions such that P is even much closer to unity. It is thus quite possible that *almost every* data values satisfy the stated Gaussian behaviour, this assumption being violated only by a small number of highly erroneous measurements. In this case one wishes to detect and eliminate them. Nevertheless P can be very close to unity for other reasons than the presence of a small number of outliers: for example this fact can also result from systematic measurements errors. In this case the illness is more serious as it affects all (or at least a large number of) measurements and not a small part of them.

Scanning data to find outliers. Here we present a way of detecting *a posteriori* the outlier(s), if any; it relies upon an *a posteriori* scanning of the data values using the χ^2 test as explained below. The whole inversion procedure would be, schematically, as follows:

(i) Inversion of the whole data set.

(ii) Computation of P defined by (2.36) and test: $P \geq P_{\mathrm{ref}}$? (with e.g. $P_{\mathrm{ref}} = 0.99$).

(iii) If the answer to (ii) is yes: determination of the modification of the inversion result induced by eliminating one data value. This step is performed sequentially for each individual datum d_i^{obs} (i taking successively the values 1, 2, ..., m) for which the solution $\langle \mathbf{m} \rangle_i'$, the covariance, matrix $\mathbf{C}_i'$ and the probability P_i' resulting from the inversion of the $m - 1$ remaining measurements are computed. We seek the value I of the index i for which $P - P_i'$ is greatest.

(iv) The datum isolated using the previous criterion is *eliminated* together with the corresponding row of $\mathbf{G}$, and the test (ii) is applied to the probability $P' = P_I'$.

→ If the answer to this test is yes, m is replaced by $m - 1$, the scanning (iii) is performed again on the remaining data and another data value is isolated and suppressed in the same way, and so on.

→ If not, end of the scanning.

If this procedure succeeded in isolating a smaller number of data values so that the inversion result *after elimination of these data values satisfies* the χ^2 test, this result is considered as the final inversion result. Otherwise other causes of violation of the gaussian assumption must be looked for.

For this method to have practical interest, the phase (iii) (scanning of the data) must not require a too large amount of computer time: performing a complete inversion for each incomplete data set is obviously out of question. Instead, we propose to use certain algebraic relations which allow to compute cheaply the result of the inversion of $m - 1$ data values by updating the result of the inversion of the whole data set.

We present our algebraic updating identities which relate the state "$m - 1$" to the state "m". For this purpose, let us give the index 1 to any quantity resulting from the treatment of the whole data set, while the index 0 denotes those corresponding to the elimination of one data value. Moreover we denote by d the (scalar) data value currently eliminated, by $\mathbf{g}$ the corresponding row of the linear operator $\mathbf{G}$ and by σ the standard deviation associated to the data value d.

From an algebraic standpoint, the states 0 and 1 can be respectively viewed as *a priori* and *a*

posteriori states. Accordingly, equation (2.4a) is applicable between the states 0 and 1, leading to:

$$\mathbf{C}_1^{-1} = \mathbf{C}_0^{-1} + \frac{1}{\sigma^2}\mathbf{g}^*\mathbf{g} \tag{2.38}$$

in which one has to keep in mind that $\mathbf{g}$ denotes a *row* vector $\mathbf{g}^*$ a *column* vector. From relation (2.38) it is possible to express $\mathbf{C}_0$ in terms of $\mathbf{C}_1$ using the *modification formula* [15]:

$$(\mathbf{A} - \mathbf{u}\mathbf{v}^*)^{-1} = \mathbf{A}^{-1} + \alpha\mathbf{A}^{-1}\mathbf{u}\mathbf{v}^*\mathbf{A}^{-1} \qquad \text{with} \qquad \alpha = \frac{1}{1 - \mathbf{v}^*\mathbf{A}^{-1}\mathbf{u}} \tag{2.39}$$

in which $(\mathbf{u},\ \mathbf{v})$ are two column vectors and $\mathbf{A}$ is a square inversible matrix; obviously the matrix $\mathbf{A} - \mathbf{u}\mathbf{v}^*$ also has to be inversible. This modification formula applied to $\mathbf{A} = \mathbf{C}_1^{-1}$, $\mathbf{u} = \mathbf{g}^*$ and $\mathbf{v}^* = \mathbf{g}/\sigma$ gives, using (2.38):

$$\mathbf{C}_0 = \mathbf{C}_1 + \frac{1}{\sigma^2 - \mathbf{g}\mathbf{C}_1\mathbf{g}^*}(\mathbf{C}_1\mathbf{g}^*)(\mathbf{C}_1\mathbf{g}^*)^* \tag{2.40}$$

Then, from formula (2.40), $\langle\mathbf{m}\rangle_0$ and $2S(\langle\mathbf{m}\rangle_0)$ can be expressed in terms of $\langle\mathbf{m}\rangle_1$ and $2S\langle\mathbf{m}\rangle_1)$ [3]; the result is:

$$\langle\mathbf{m}\rangle_0 = \langle\mathbf{m}\rangle_1 + \frac{\mathbf{g}\langle\mathbf{m}\rangle_1 - d}{\sigma^2 - \mathbf{g}\mathbf{C}_1\mathbf{g}^*}\mathbf{C}_1\mathbf{g}^* \tag{2.41}$$

$$2S(\langle\mathbf{m}\rangle_0) = 2S(\langle\mathbf{m}\rangle_1) - \frac{1}{\sigma^2 - \mathbf{g}\mathbf{C}_1\mathbf{g}^*}(\mathbf{g}\langle\mathbf{m}\rangle_1 - d)^*(\mathbf{g}\langle\mathbf{m}\rangle_1 - d\rangle \tag{2.42}$$

Then the following difference is computed in step (iii) of the scanning algorithm:

$$P_1 - P_0 = P(\chi^2(2m) \leq 2S(\langle\mathbf{m}\rangle_1)) - P(\chi^2(2m-2) \leq 2S(\langle\mathbf{m}\rangle_0)) \tag{2.43}$$

and the data value associated to the greatest value $P_1 - P_0$ encountered during the scanning is eliminated.

The solution $(\langle\mathbf{m}\rangle_1,\ 2S(\langle\mathbf{m}\rangle_1))$ of the Gaussian inversion method is updated and takes the values $(\langle\mathbf{m}\rangle_0,\ 2S(\langle\mathbf{m}\rangle_0))$ given by the equations (2.41) and (2.42) and corresponding to the datum actually suppressed. The covariance matrix is not updated using (2.40) since the "one-by-one" inversion algorithm described in section 2.3 as well as the confidence indicators manipulate only $\mathbf{C}^{1/2}$, which will be updated instead. The equation (2.40) can be rewritten as:

$$\mathbf{C}_0 = \mathbf{C}_1^{*/2}\left[\mathbf{I} + \beta\left[\mathbf{C}_1^{1/2}\mathbf{g}\right]\left[\mathbf{C}_1^{1/2}\mathbf{g}\right]^*\right]\mathbf{C}_1^{1/2} \qquad \text{with} \qquad \beta = \frac{1}{\sigma^2 - \left[\mathbf{C}_1^{1/2}\mathbf{g}\right]^*\left[\mathbf{C}_1^{1/2}\mathbf{g}\right]} \tag{2.44}$$

Then we use, in a way similar to section 4.3, the fact that an exact expression of the Choleski decomposition of a matrix $\mathbf{T}$ of the form: $\mathbf{T} = \mathbf{I} + \alpha\mathbf{v}\mathbf{v}^*$ (which is clearly positive definite) is known:

$$\mathbf{T} = \mathbf{T}^{*/2}\mathbf{T}^{1/2} \quad \text{with} \quad \left(\mathbf{T}^{1/2}\right)_{ii} = \left(\frac{1 + \alpha s_i}{1 + \alpha s_{i-1}}\right)^{1/2}, \quad \left(\mathbf{T}^{1/2}\right)_{ij} = \frac{\alpha \mathbf{v}_i \bar{\mathbf{v}}_j}{((1 + \alpha s_i)(1 + \alpha s_{i-1}))^{1/2}} \tag{2.45}$$

$$s_i = v_1^* v_1 + \ldots + v_i^* v_i$$

This result, applied to $\alpha = \beta$ and $\mathbf{v} = \mathbf{C}_1^{1/2}\mathbf{g}^*$, yields the transfer relation between $\mathbf{C}_0^{1/2}$ and $\mathbf{C}_1^{1/2}$:

$$\mathbf{C}_0^{1/2} = \mathbf{T}^{1/2}\mathbf{C}_1^{1/2} \tag{2.46}$$

and allows the updating of $\mathbf{C}^{1/2}$.

Thus the algebraic transfer identities (2.41), (2.42) and (2.46) allow one to perform the *a posteriori* scanning of the data set and the updating of the quantities produced by Gaussian inversion *at a small extra computational cost*. These identities are a consequence of the modification formula (2.39) which allows the updating of the inverse of a matrix undergoing a *small rank* perturbation (here, a rank one perturbation) at an algebraic operations cost *small compared to that required for a whole matrix inversion*.

3. Application of the Gaussian inversion method to the acoustical inverse problem: numerical results.

In this part we examine on an example the numerical results obtained by this approach of the inverse problem. This example is "synthetic", the data (pressure values at measurement points) being computed numerically for a certain normal velocity field, using integral equation (1.11) and representation (1.12) *via* our boundary element code TRIAC installed at LMS.

• Geometry and vibratory motion. — An orthogonal cartesian coordinate system $(Oxyz)$ is attached to the three-dimensional geometrical space, in which we consider a cylindrical surface (S) (axis Oz, radius $R = 1$ m, bounded by the planes $z = \pm 3m$), set into a vibratory motion of normal velocity U given, in cylindrical coordinates (r, θ, z), by:

$$\begin{array}{lll} U(\theta, z) = \cos^2\theta\cos^2(\pi z/3) & \text{if } |z| \leq 1.5 & \text{and} \quad -\pi/2 \leq \theta \leq \pi/2 \\ U(\theta, z) = 0. & \text{otherwise} & \end{array} \tag{3.1}$$

This expression for U is chosen in order to test the ability of the inversion method to reconstruct a normal velocity field of relatively small support. In the sequel the numerical tests will be done for the two values $kR = 0.5$ and $kR = 2.$ of the non-dimensional frequency.

• Measurement points. — We consider two sets of 282 measurement points, at which the radiated pressure is known, defined as follows (Fig. 7):

- two regular square grids (G1) and (G2) of size $a_y \times a_z$, each containing $11^2 = 121$ regularly spaced points, located in the planes $x = \pm x_0$, centered with respect to the coordinate axis Ox and with sides parallel to Oy and Oz.
- The 40 remaining points are located on a square (C) $((|y| - a_y)(|z| - a_z) = 0,\ x = 0)$, dividing each side into 10 constant subintervals.

The two sets of measurement points correspond respectively to $(x_0 = 5.,\ a_y = a_z = 5.)$ and $(x_0 = 1.25.,\ a_y = 1.25,\ a_z = 3.25)$. They can be considered respectively as *far-field* and *near-field* measurement sets, and accordingly will be denoted (FF) and (NF) respectively.

• Data uncertainties. — The real and imaginary parts of the "measured" pressure values have been given a standard deviation $\sigma_D = 10^{-3} \times$ (measured value).

• Boundary element discretization. — S is approximated by 54 eight-noded quadratic boundary elements (9 elements for each of the top and bottom faces and 36 for the lateral face), for a total of 164 pressure nodes and 188 normal velocity nodes (these two numbers being different due to the edges $z = \pm 3,\ r = 1$). The unknowns for the inverse problem are then the 188 nodal values for the normal velocity U. The linear discretized operator G is built using the code TIRAC. The direct linear operator G is thus a 282×188 complex fully-populated and unstructured matrix, which is a large size for an ill-posed problem.

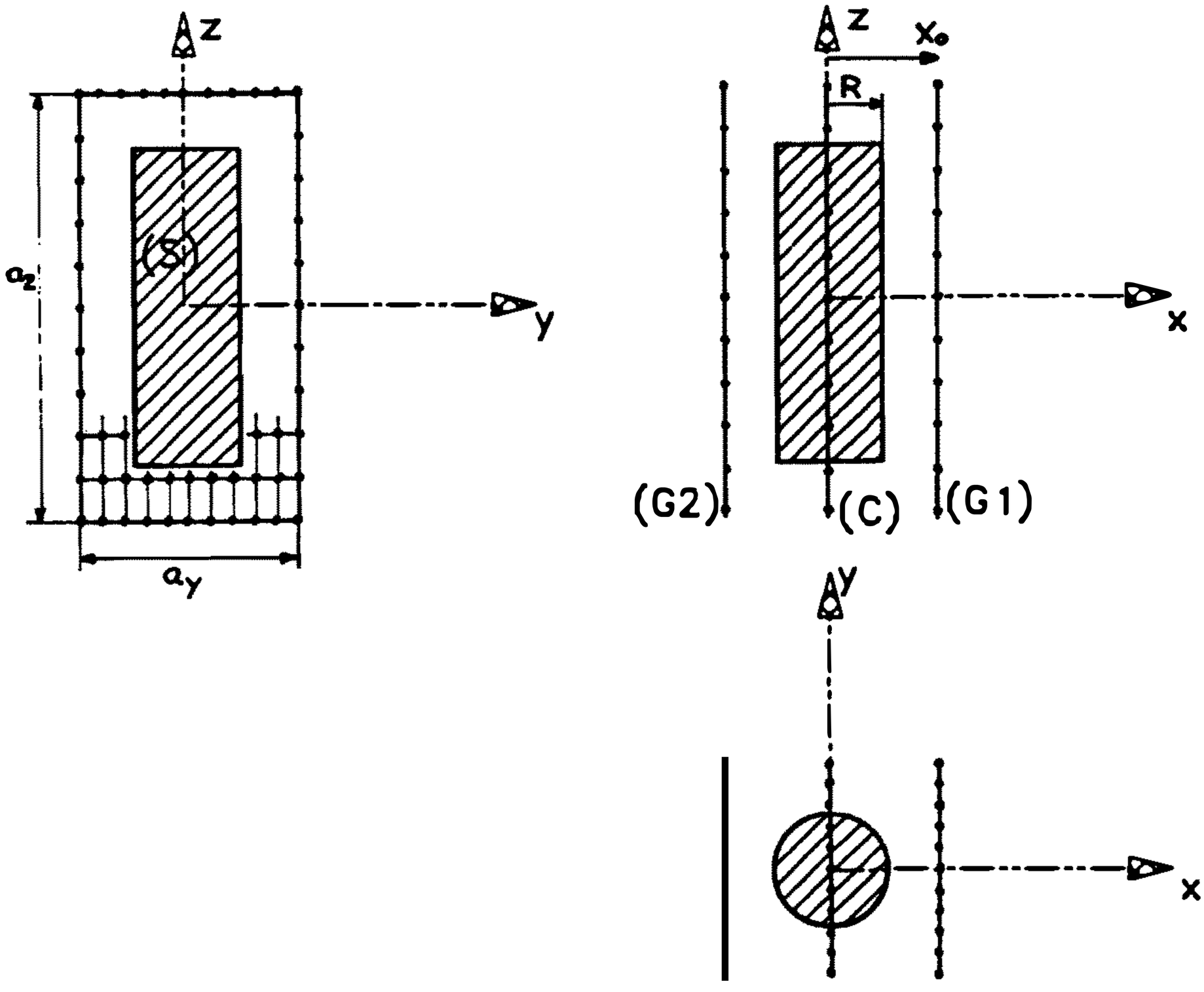

Fig. 7. — Vibration of a cylinder and measurement points: geometrical configuration.

We will examine the influence on the inversion results of (a) the choice of *a priori* information (here, σ_M and L), (b) the presence of outliers, (e) random perturbations of the measurements. We present (d) the results given by the confidence indicators (mean standard diviation, relative information IR, resolution coefficient r). Finally we give in (a) and (c) some comparisons between the results obtained using ordinary least squares and Gaussian inversion. The computer time spent to perform one inversion is 910s on a wokstation HP-APOLLO DN 400, with maximum optimization of the code by the compiler.

As a first remark, we performed a singular value decomposition on G for the two measurement sets and the two frequencies, using the above-mentioned LINPACK [15] routine CSVDC. CSVDC failed to give any correct singular value in the far-field case, whereas it gave *all* the singular values in the near-field case. In the latter case, we obtain Cond(G)= 8.16×10^5 (for $kR = 0.5$) and Cond(G) = 1.28×10^5 (for $kR = 2$); the CPU time spent was approximately 1300s on a work-station HP-APOLLO DN400, that is, more than the time needed for a Gaussian inversion with the same matrix G. Thus the singular value decomposition technique could not be applied to the present problem in the far-field case. These numerical results match the conclusions of the study of the sphere problem done in section 1.

(a) Choice of *a priori* information. — In analogy with the method proposed by Tarantola for the Gaussian inversion of infinite-dimensional linear inverse problems [10], covariance matrices of the following type have been used:

$$(\mathbf{C_M})_{ij} = \sigma_M^2 \exp\left(\frac{1}{L}\,\|\mathbf{x}_i - \mathbf{x}_j\|_S\right) \tag{3.2}$$

that is, a discrete version of the exponential covariance function (see [10] or [11]). The distance $\| \ \|_S$ appearing in (3.2) is the distance *along the surface S*, L denoting some characteristic length considered to be relevant (e.g. a vibration "wavelength" characteristic of the motion of S considered as an elastic structure) and σ_M a standard deviation (which physical dimension here is a velocity). The smaller σ_M, the greater weight of this information for the inversion process. The covariance (3.2) thus expresses that two nodes on S are correlated if their distance along S is not large compared to a characteristic "correlation length" L. A choice such as (3.2) is not mandatory but provides a good way of introducing a physical *a priori* information, namely the correlation length L.

On the other hand $\mathbf{m}_{prior}$ has been chosen as the vector of equal components which satisfies at best (in a least squares sense) the measurements.

The figures 8 to 11 plot the quadratic error between the "exact" (in the sense of (3.1)) and computed nodal values of U against the correlation length L, for the two measurement sets and the two frequencies considered; here the simulated data is exact (no noise addition). These results show that the Gaussian inversion behaves very differently in the far-field (Figs. 8, 9) and the near-field (Figs. 10, 11) cases. In the former case the results are poor for $L < 2.$, which confirms the interest of this *a priori* information when the inverse problem is ill-posed (a value typical of the problem considered, according to (3.1), could be $L = 3.$), whereas in the latter case, which is less ill-posed, the results are better for small values of L and their accuracy is very dependent on the weight σ_M given to C_M.

Figure 12 shows the real part of the nodal values $U(\mathbf{x}_i)$ at the nodes $\mathbf{x}_i$ located on the generator ($x = 1,\ y = 0$) of S, bracketed between the values $\mathrm{Re}[U(\mathbf{x}_i)] \pm (C_{ii}/2)^{1/2}$ (for this example we used the far-field measurement set together with $kR = 0.5,\ \sigma_M = 1$).The quantity $(C_{ii}/2)^{1/2}$ is, according to the discussion of section 2.3, the standard deviation associated to either the real or imaginary part of $U(\mathbf{x}_i)$; the magnitude of the $(C_{ii}/2)^{1/2}$ $(i = 1, \ldots, n)$ define one confidence indicator related to the reconstructed values of U. One can see on this particular example that the value $\sigma_M = 1$, defining too narrow *a priori* "soft bounds" on m, seems responsible of the poor "peak" value of U at $z = 0$ in figure 12, which contributes greatly to the overall reconstruction error.

(b) Presence of outliers. — The scanning algorithm described in section 2.4 has been tested: we performed a Gaussian inversion in which an error of approximately 10% has been added to the measurements 76, 77 and 78.

The figure 13 shows both the extreme sensitivity of the solution to such outliers and the efficiency of the scanning algorithm. Our Gaussian inversion program succeeded in finding and eliminating those outliers, and only them, and in updating the solution. On this example, the extra computer time spent in scanning the data set and eliminating the outliers was approximately 10% of the "normal" inversion computer time for the same problem.

(c) Influence of random perturbations of the measurements. We compared the results given by the ordinary leastsquares method (Householder reduction, programs CQRDC and CQRSL from the software library LINPACK [15]) and the gaussian inversion. The "measured" values have been given, as before, a standard deviation $\sigma_D = 10^{-3}\times$ (measured value). The measurements were perturbed by adding to them the realisation of a Gaussian random variable of standard deviation $\sigma_p \times$ (measured value). Inversions have been performed for several values of σ_p, the quadratic error for the nodal values of U is displayed against σ_p for the two inversion methods in the tables I to IV.

In the far-field case (Tabs. I and II), the results show that the ordinary least squares inversion produces correct results for exact data only. In this latter case, the results are better than using Gaussian inversion, which is not surprinsing since, contrarily to the Gaussian inversion, there is

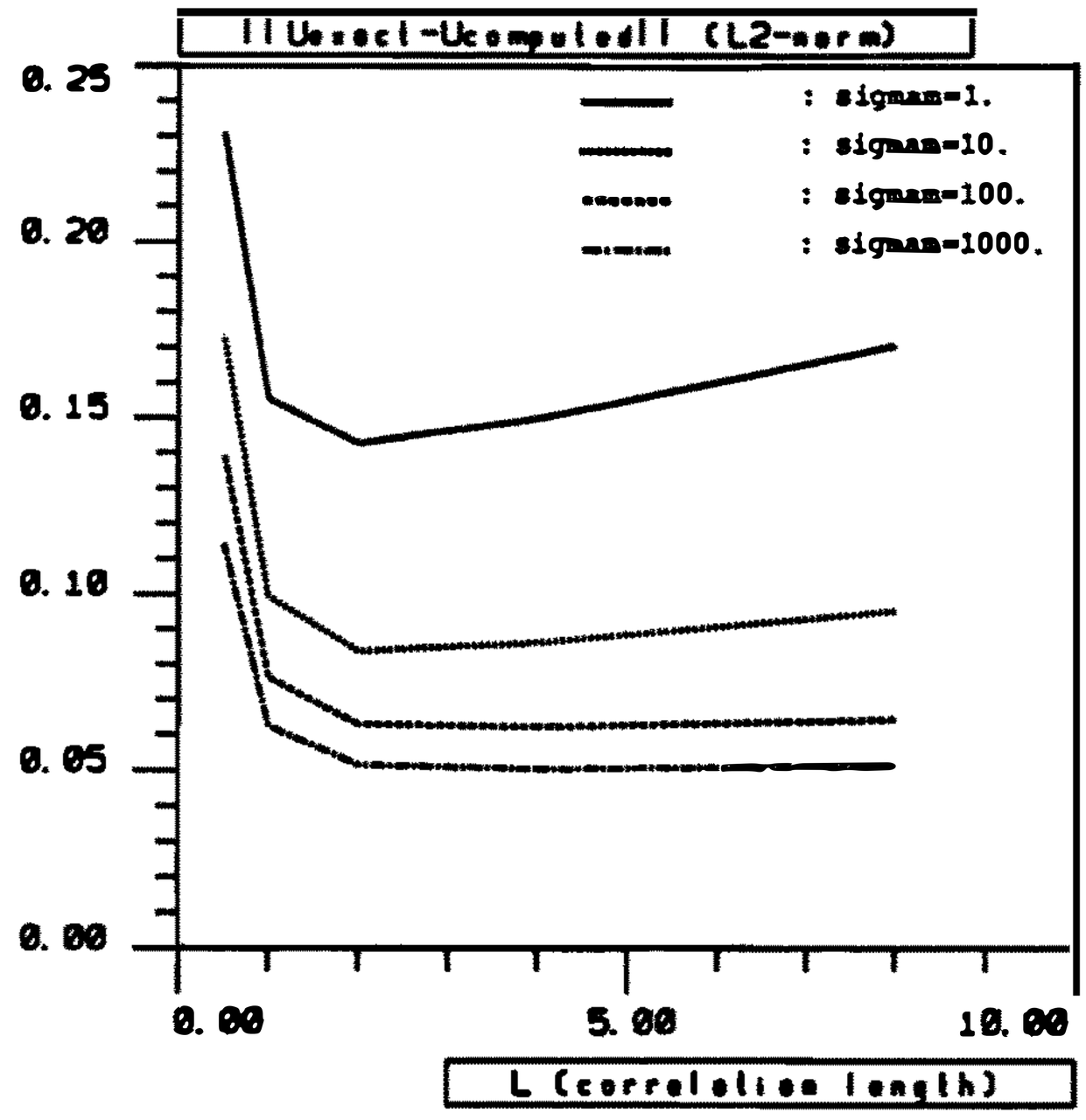

Fig. 8. — Quadratic relative error between "exact" (given by (3.1)) and computed (by means of Gaussian inversion) nodal values of U, against L and for several values of σ_M : case ((FF), $kR = 0.5$).

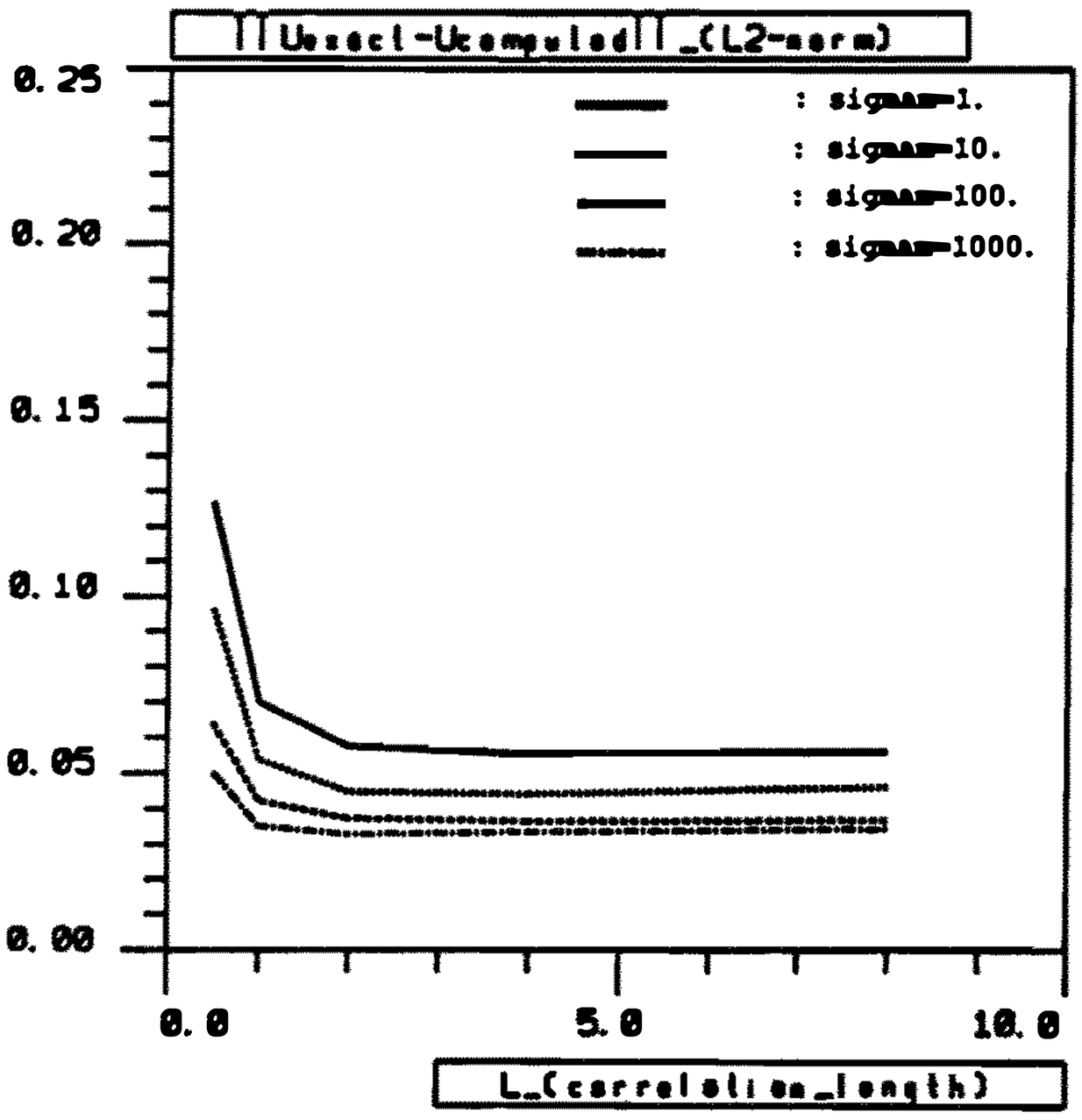

Fig. 9. — Quadratic relative error between "exact" (given by (3.1)) and computed (by means of Gaussian inversion) nodal values of U, against L and for several values of σ_M : case ((FF), $kR = 2.$).

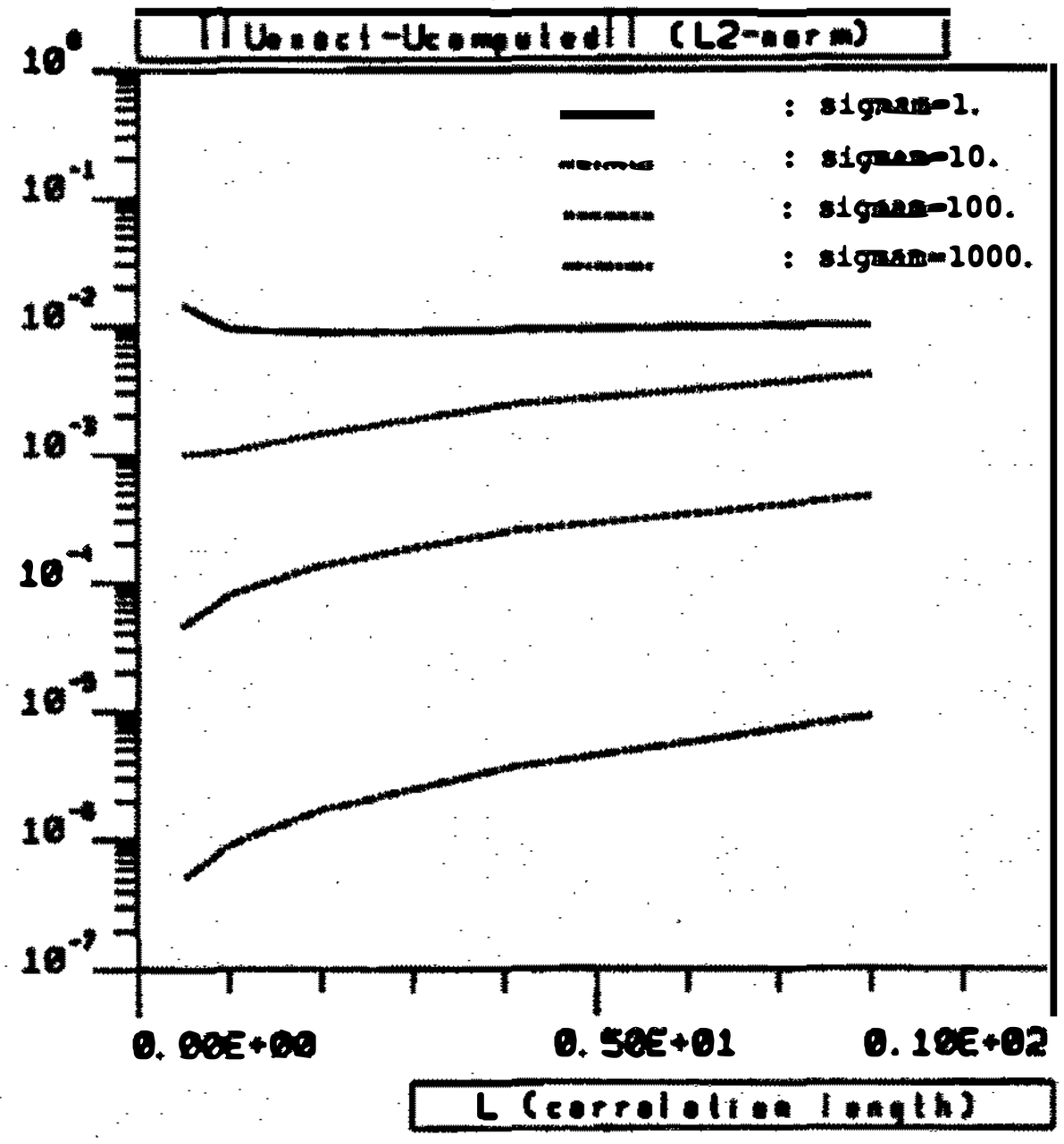

Fig. 10. — Quadratic relative error between "exact" (given by (3.1)) and computed (by means of gaussian inversion) nodal values of U, against L and for several values of σ_M : case ((NF), $kR = 0.5$).

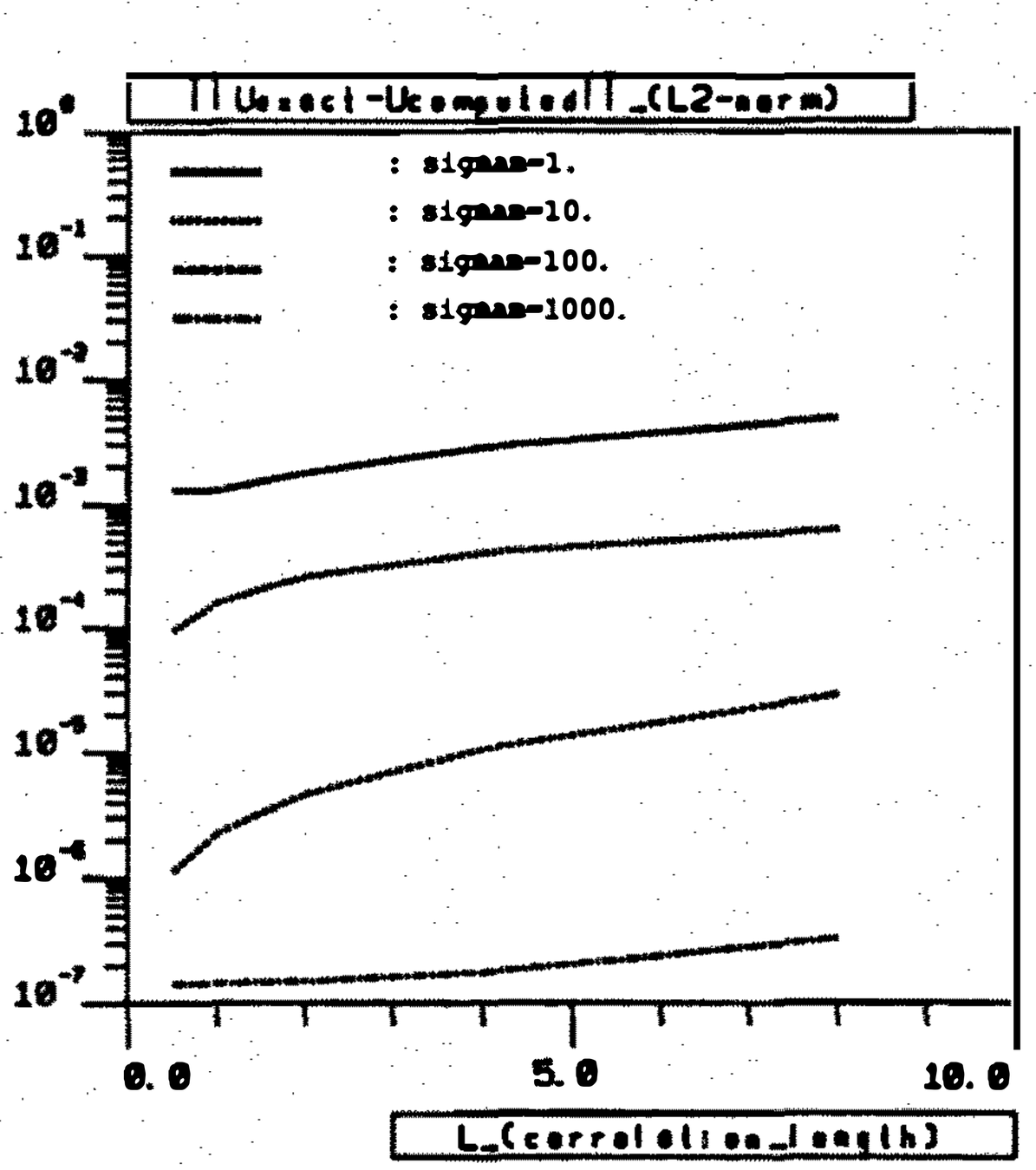

Fig. 11. — Quadratic relative error between "exact" (given by (3.1)) and computed (by means of gaussian inversion) nodal values of U, against L and for several values of σ_M : case ((NF), $kR = 2.$).

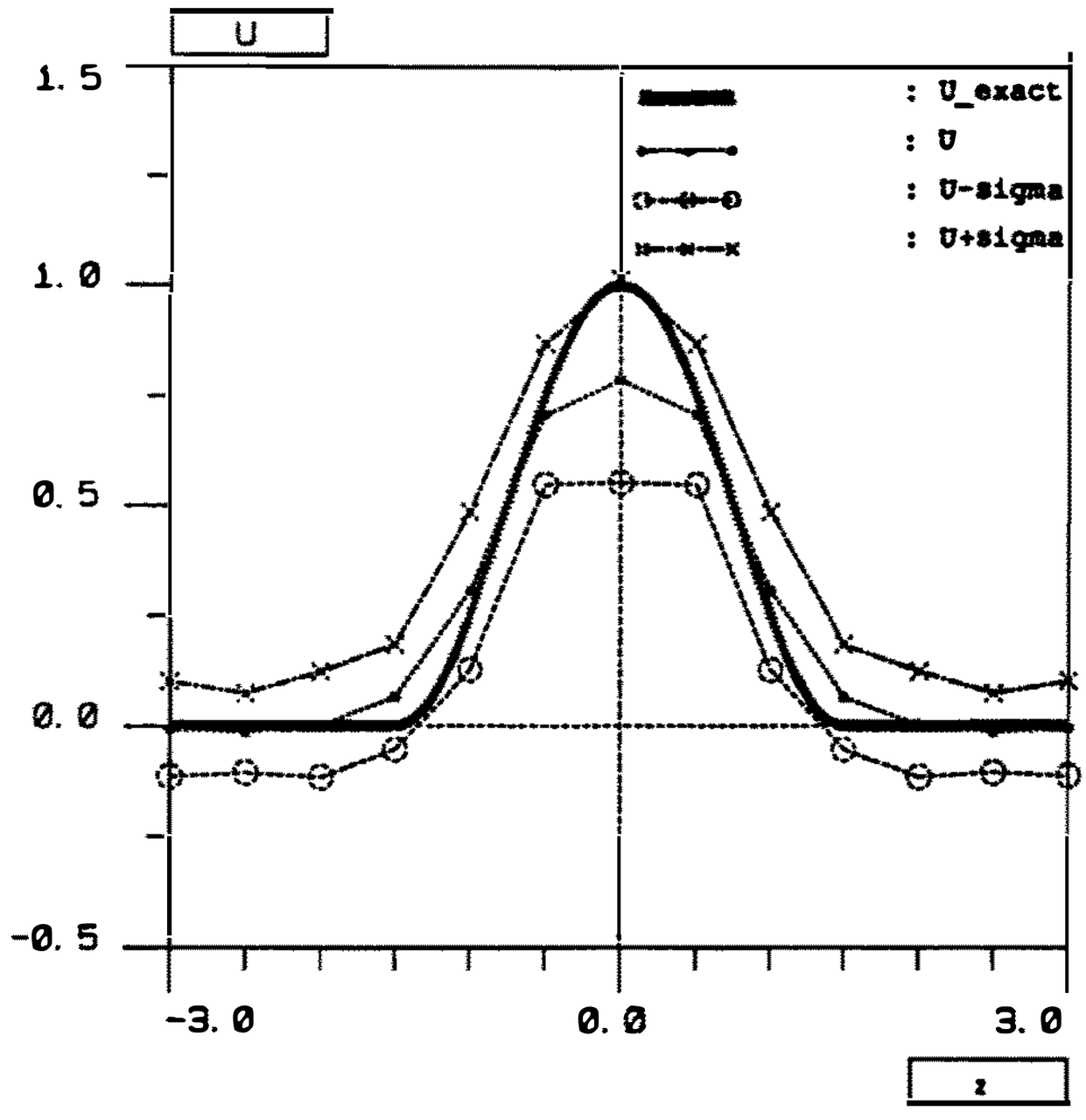

Fig. 12. — Nodal values $U(\mathbf{x}_i)$ at the nodes located on the generator ($x = 1,\ y = 0$) of S, and upper and lower bounds $(\mathbf{x}_i) \pm (C_{ii}/2)^{1/2}$. This is one confidence indicator related to the reconstructed values of U.

no compromize between fitting the data and satisfying some *a priori* information. On the contrary, on the present example, any noise completely deteriorates the results obtained by ordinary least squares while the gaussian inversion shows more stability with respect to random fluctuations.

Table I. — *Comparison of quadratic errors for reconstructions performed using least-squares and Gaussian inversion, against the relative standard deviation σ_p of the noise added to the data (far-field measurement case, $kR = 0.5$).*

	Gaussian inversion		least squares	
	L^2 error	$P(2.37)$	L^2 error	$P(2.37)$
$\sigma_p = 0.$	0.14	0.	0.0080	0.
$\sigma_p = 10^{-5}$	0.093	0.	3.6×10^{6}	6.1×10^{-122}
$\sigma_p = 10^{-4}$	0.15	0.	3.6×10^{7}	4.0×10^{-75}
$\sigma_p = 10^{-3}$	0.39	2.0×10^{-42}	3.6×10^{8}	5.6×10^{-30}
$\sigma_p = 10^{-2}$	2.08	1.	3.6×10^{9}	0.60
$\sigma_p = 10^{-1}$	2.52	1.	3.6×10^{10}	1.

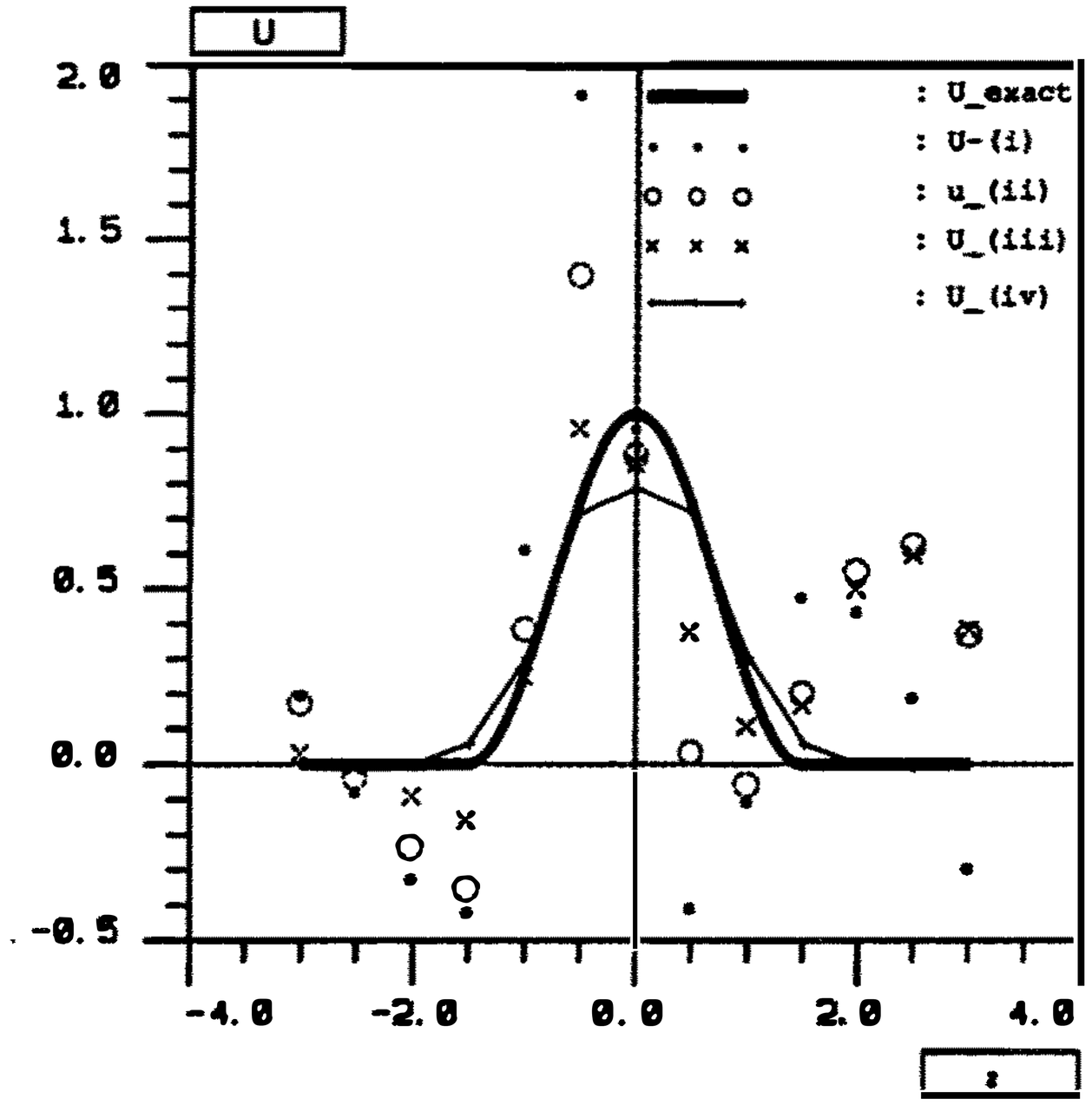

Fig. 13. — Nodal values of U, for the same nodes as figure 3.2, after automatic detection and suppression of experimental values (i) none (ii) 78 (iii) 78, 77 and (iv) 78, 77 et 76 by the algorithm.

Table II. — *Comparison of quadratic errors for reconstructions performed using least-squares and Gaussian inversion, against the relative standard deviation σ_p of the noise added to the data (far-field measurement case, $kR = 2.$).*

	Gaussian inversion		least squares	
	L^2 error	$P(2.37)$	L^2 error	$P(2.37)$
$\sigma_p = 0.$	0.058	0.	7.2×10^{-4}	0.
$\sigma_p = 10^{-5}$	0.058	0.	9.1×10^{4}	1.3×10^{-122}
$\sigma_p = 10^{-4}$	0.064	0.	9.1×10^{5}	8.8×10^{-76}
$\sigma_p = 10^{-3}$	0.28	7.6×10^{-54}	9.1×10^{6}	1.4×10^{-30}
$\sigma_p = 10^{-2}$	1.41	1.	9.1×10^{7}	0.51
$\sigma_p = 10^{-1}$	2.38	1.	9.1×10^{8}	1.

In the near-field case (Tabs. III and IV), the same comments hold, but the compared behaviour of the two methods is not as radically different as in tables I and II.

In both cases, one can see that the stability of gaussian inversion strongly deteriorates when $\sigma_p \geq \sigma_D$.

(d) Results given by the confidence indicators. — Let us compare the results obtained in reconstructing U for the two measurements sets (FF), (NF) and the two frequencies $kR = 0.5, 2.$

Table III. — *Comparison of quadratic errors for reconstructions performed using least-squares and Gaussian inversion, against the relative standard deviation* σ_p *of the noise added to the data (far-field measurement case,* $kR = 0.5$).

	Gaussian inversion		least squares	
	L^2 error	$P(2.37)$	L^2 error	$P(2.37)$
$\sigma_p = 0.$	0.0086	0.	1.6×10^{-7}	0.
$\sigma_p = 10^{-5}$	0.0089	0.	0.23	1.0×10^{-121}
$\sigma_p = 10^{-4}$	0.024	0.	2.27	1.6×10^{-75}
$\sigma_p = 10^{-3}$	0.23	8.4×10^{-98}	22.7	8.7×10^{-30}
$\sigma_p = 10^{-2}$	1.37	1.	227.	0.63
$\sigma_p = 10^{-1}$	2.09	1.	2271	1.

Table IV. — *Comparison of quadratic errors for reconstructions performed using least-squares and Gaussian inversion, against the relative standard deviation* σ_p *of the noise added to the data (far-field measurement case,* $kR = 2.$).

	Gaussian inversion		least squares	
	L^2 error	$P(2.37)$	L^2 error	$P(2.37)$
$\sigma_p = 0.$	0.0018	0.	1.6×10^{-7}	0.
$\sigma_p = 10^{-5}$	0.0033	0.	0.022	8.7×10^{-122}
$\sigma_p = 10^{-4}$	0.024	0.	0.22	5.6×10^{-75}
$\sigma_p = 10^{-3}$	0.24	1.8×10^{-93}	2.18	7.7×10^{-30}
$\sigma_p = 10^{-2}$	1.25	1.	21.8	0.62
$\sigma_p = 10^{-1}$	2.37	1.	218.	1.

considered. Table V displays, for each case, the quadratic error for the normal velocity nodal values ("L^2 error"), the relative information for the overall inversion (IR, given by (2.34)), the geometrical mean $\langle \sigma^{post} \rangle$ of the *a posteriori* standard deviations associated to the unknowns and the resolution coefficient r (2.15). The measurements have been given a standard deviation equal to $10^{-3} \times$ (measured value). Besides, $\sigma_M = 10.$ and $L = 2.$. One can see that the three indicators displayed vary according to the actual precision of the result and give concordant indications about the quality of the result. This illustrates the interest of such indicators in practical cases, for which the actual precision is obviously not known. An important remark concerning the interpretation of $\langle \sigma^{post} \rangle$ and r is that these quantities *are independent of the data values* $\mathbf{d}_{obs}$ (see (2.7) and (2.14)); they are related to the resolving power of the *physical model* G. On the contrary, IR depends on G *and* on $\mathbf{d}_{obs}$ (through the result $\langle \mathbf{m} \rangle$).

Table V. — *The confidence indicators IR, $\langle\sigma^{post}\rangle$ and r are displayed together with the actual L^2 error for the two measurement sets and the two frequencies considered.*

	$kR = 0.5$ (FF)	$kR = 2.$ (FF)	$kR = 0.5$ (NF)	$kR = 2.$ (NF)
L^2 error	8.36×10^{-2}	4.48×10^{-2}	1.4410^{-3}	2.610^{-4}
IR (2.20)	1.09×10^{-3}	2.49×10^{3}	3.8810^{3}	4.8410^{3}
$\langle\sigma^{post}\rangle$	0.57	0.080	0.010	2.810^{-3}
r(2.15)	0.316	0.523	0.908	0.976

4. Conclusions.

In this paper, the inverse problem of recovering the normal velocity of a vibrating surface using pressure measurements (a procedure which is sometimes known as "acoustic holography") has been adressed. We were primarily interested in studying its ill-posed character.

In section 1 the well-known problem of the vibrating sphere was considered, in order to study the condition number of the problem on the truncated analytical solution. This investigation showed that the acoustic holography problem may be ill-conditioned, especially for far-field measurements and/or low frequencies.

Section 2 was devoted to the exposition of the Gaussian inversion concept and of the specific algorithm developed, the Gaussian inversion approach being designed to solve numerically ill-posed discrete inverse problems. Our algorithmic development focused on the practical obtention of interpretable confidence indicators on the inversion result, the interpretation of complex-valued Gaussian random variables and the automatic detection of outliers. Although the basic concept of gaussian inversion has been formulated by Tarantola [10], some of the developments in this section are new, to the best of our knowledge.

In section 3 we tested numerically our algortihm on a particular problem, namely a vibrating cylinder, using simulated data. The numerical physical model relating the acoutical pressures to the vibratory motion was built using a boundary element discretization of the cylinder and the classical integral representation formula; for this purpose we used our boundary element code TRIAC. This method allows one to perform numerical acoustical holographies for abitrary vibrating surfaces. We chose a rather fine discretization, leading to a discrete inverse problem of rather large size (282 measurements and 188 unknowns) in order to study the behaviour of our method for large-size problems. The results of these tests, regarding the ill-conditioning, confirm the predictions of the preliminary investigation of section 1. We noticed that the ordinary least-squares method (using the Householder factorization) gives more accurate results for exact data but performs poorly for far-field measurements if the data experience a slight random perturbation. Moreover, the singular value decomposition algorithm available in the software library LINPACK failed to give any correct singular value in the case of far-field measurements, which prevents one to use for this case the truncated singular value decomposition as was done in some recent works on the same subject. The numerical results show the interest of the computed confidence indicators. Finally our algorithm for finding outliers performs very well.

As a general conclusion, we showed the applicability and interest of the gaussian inversion approach applied to acoustic source inverse problems, especially in cases where the problem is ill-posed. The robustess of the Gaussian inverison method is obtained at the expense of a loss of accuracy (compared to the ordinary least squares method) if the data happen to be exact, but this

is very unlikely to occur for practical problems.

The present algorithm itself is not specifically designed towards acoustic holography problems, it can solve anylinear discrete complex-valued inverse problem. It is nowused by the Departement Acoustique et Mécanique Vibratoire of Electricité de France for various identification problems.

Acknowledgements.

This work has been done as a part of a reseasrch convention between Electricité de France (dept. Acoustique et Mécanique Vibratoire) and the Laboratoire de Mécanique des Solides of Ecole Polytechnique [11], [12]. The author thanks Thierry Balannec and Emile Luzzato of Electricité de France for numerous useful discussions.

References

[1] MAYNARD J. D., WILLIAMS E. G. and LEE Y., Near-field acoustic holography: theory of generalized holography and the development of NAH, *J. Acoust. Soc. Am.* **78** (1985) 1395-1413.

[2] VERONESI W. A. and MAYNARD J. D., Digital holographic reconstruction of sources with arbitrarily shaped surfaces, *J. Acoust. Soc. Am.* **85** (1989) 588-598.

[3] BORGIOTTI G. V., SARKISSIAN A., WILLIAMS E. G. and SCHUETZ L., Conformal generalized near-field acoustic holography of axisymmetric geometries, *J. A coust. Soc. Am.* **84** (1988) 385-391.

[4] BREBBIA C. A., TELLES J. C. F., WROBEL L. C., Boundary Element Techniques, Theory and Application in Engineering (Springer - Verlag, 1984).

[5] COLTON D. and KRESS R., Integral Equation Method in Scattering Theory (John Wiley & sons, 1983).

[6] FILIPPI P. J. T., Integral equations in acoustics, Theoretical acoustics and numerical techniques, P. J. T. Filippi Ed. (Springer-Verlag, 1983).

[7] SHAW R. P., Acoustics, In "Boundary element methods in mechanics", D. E. Beskos Ed. (North Holland, 1987).

[8] AUDOLY C., Sur l'utilisation de l'holographie acoustique pour les antennes d'émission, Rapport DCN Toulon n° 061208, 1989.

[9] AUDOLY C., Determination of the transducer velocities in a sonar array using digital acoustical holography, 1er congrès d'Acoustique, *J. Phys. Colloq. France* **51** (1990) C2.

[10] TARANTOLA A., Inverse problem theory (Elsevier, 1987).

[11] BONNET M., Un aperçu des approches existantes pour la description mathématique et la résolution des problèmes inverses, Rapport contrat EDF et Note interne N° 14, Laboratoire de Mécanique des Solides, 1989.

[12] BONNET M., Détermiantion, par inversion stochastique des mesures de champ de presson rayonnée, de caractéristiques vibratoires d'une machine, Rapport contrat EDF, septembre 1990.

[13] MORSE Ph. M and INGARD K. U., Theoretical acoustics (Mc Graw Hill).

[14] GRADSHTEYN I. S. and RYZHIK I. M., Tables of integrals, series and products (Academic Press, 1980).

[15] DONGARRA J. J., BUNCH J. R., MOLER C. B. and STEWART G. B., LINPACK users' guide, SIAM. Philadelphia (1979).

[16] RIZZO F. J., SHIPPY D. J. and REZAYAT M., A boundary integral equation method for radiation and scattering of elastic waves in three-dimensions, *Int. J. Num. Meth. Eng.* 21 (1985) 115-129.

[17] BONNET M., Méthode des équations intégrales régularisées en élastodynamique tridimensionnelle. Thèse de doctorat, Bulletin EDF/DER série C, n° 1/2, 1987.

[18] MENKE W., Geophysical data analysis: discrete inverse theory (Academic Press, 1984).

[19] SABATIER P. C., problèmes inverses et applications; Cours Ecole d'Eté d'Analyse Numérique (CEA - INRIA -EDF) 1985.

[20] LAVRENTIEV M. M., Some improperly posed problems of mathematical physics (Springer-Verlag, Berlin, 1987).

[21] TIKHONOV A. and ARSENINE V., Méthodes de résolution de problèmes mal posés (Editions Mir, 1976).

[22] LATTES R. and LIONS J. L., Méthode de quasi-réversibilité et applications. Dunod (Paris), 1967.

[23] LUZZATO E., L'inversion dans des espaces de dimension infinie. Note interne EDF/DER.
[24] PRESS W. H., FLANNERY B. P., TEUKOLSKY S. A. and VETTERLING W. T., Numerical recipes: the art of scientific computing (Cambridge press, 1986).
[25] HAGER W. W., Updating the inverse of a matrix, *SIAM Rev.* **31** (1989) 221-239.